



Published in final edited form as:

Synapse. 2019 May ; 73(5): e22088. doi:10.1002/syn.22088.

Chronic immobilization stress primes the hippocampal opioid system for oxycodone associated learning in female but not male rats

Batsheva Reich¹, Yan Zhou², Ellen Goldstein¹, Sudarshan S. Srivats³, Natalina H. Contoreggi¹, Joshua F. Kogan⁴, Bruce S. McEwen⁴, Mary Jeanne Kreek², Teresa A. Milner^{1,4,*}, Jason D. Gray^{4,*}

¹Feil Family Brain and Mind Research Institute, Weill Cornell Medicine, 407 East 61st Street, New York, NY 10065

²The Laboratory of the Biology of Addictive Diseases, The Rockefeller University, 1230 York Avenue, New York, NY 10065

³Weill Cornell Medicine in Qatar, Qatar Foundation, Education City, P.O. Box 24144 - Doha, Qatar

⁴Harold and Margaret Milliken Hatch Laboratory of Neuroendocrinology, The Rockefeller University, 1230 York Avenue, New York, NY 10065

Abstract

In adult female, but not male, Sprague-Dawley rats, chronic immobilization stress (CIS) increases mossy fiber (MF) Leu-Enkephalin levels and redistributes delta- and mu-opioid receptors (DORs and MORs) in hippocampal CA3 pyramidal cells and GABAergic interneurons to promote excitation and learning processes following subsequent opioid exposure. Here, we demonstrate that CIS females, but not males, acquire conditioned place preference (CPP) to oxycodone and that CIS “primes” the hippocampal opioid system in females for oxycodone-associated learning. In CA3b, oxycodone-injected (Oxy) CIS females relative to saline-injected (Sal) CIS females exhibited an increase in the cytoplasmic and total densities of DORs in pyramidal cell dendrites so that they were similar to Sal- and Oxy-CIS males. Consistent with our earlier studies, Sal- and Oxy-CIS females but not CIS males had elevated DOR densities in MF-CA3 dendritic spines, which we have previously shown are important for opioid-mediated long-term potentiation. In the dentate gyrus, Oxy-CIS females had more DOR-labeled interneurons than Sal-CIS females. Moreover, Sal- and Oxy-CIS females compared to both groups of CIS males had elevated levels of DORs and MORs in GABAergic interneuron dendrites, suggesting capacity for greater synthesis or storage of these receptors in circuits important for opioid-mediated disinhibition. However, more plasmalemmal MORs were on large parvalbumin-containing dendrites of Oxy-CIS males compared to Sal-CIS males, suggesting a limited ability for increased granule cell disinhibition.

*Address correspondence to: Corresponding author: Teresa A. Milner, Ph.D., Feil Family Brain and Mind Research Institute, Weill Cornell Medicine, 407 East 61st Street, RM 307, New York, NY 10065 United States of America, FAX: (646) 962-0535, tmilner@med.cornell.edu.

*Co-Senior authors

Author Contributions: T.A.M., M.J.K. and B.S.M. designed research; B.R., Y.Z., E.G., S.S.S., N.H.C., J.F.K., K.T.B., T.A.M., and J.D.G. performed research; B.R., E.G., S.S.S., N.H.C., T.A.M. analyzed data; B.R., J.D.G., T.A.M., B.S.M., M.J.K. wrote the paper.

Conflict of Interest: The authors declare no competing financial interests.

These results suggest that low levels of DORs in MF-CA3 synapses and hilar GABAergic interneurons may contribute to the attenuation of oxycodone CPP in males exposed to CIS.

Keywords

Conditioned place preference; Delta opioid receptor; Drug addiction; GABAergic interneurons; Leu-enkephalin; Mossy fiber – CA3 synapses; Mu opioid receptor

INTRODUCTION

During the last two decades, opioid use and abuse have escalated dramatically (CDC, 2015). The transition from drug use to addiction critically depends on neural circuits involved in the encoding of motivational incentives as well as associative memory formation (Koob and Volkow, 2010; Sjulson et al., 2018). Within the rodent hippocampus, opioid signaling in the CA3 subregion has been shown to play an important role in spatial memory and in contextual associative learning (Kesner and Warthen, 2010; Meilandt et al., 2004). Moreover, a form of opioid-mediated long-term potentiation (LTP) in CA3 pyramidal cells contacted by mossy fibers (i.e., mossy fiber-CA3 synapses) is present in high-estrogen state female rats but not male rats (Harte-Hargrove et al., 2015) suggesting that opioid associative learning processes could be enhanced in females in certain hormonal states. In support, cyclic fluctuations of estrogen levels have been shown to alter morphine sensitivity in women (Ribeiro-Dasilva et al., 2011) and patterns of heroin self-administration in rats (Lacy et al., 2016).

Stress is a crucial factor in multiple aspects of addiction, including relapse (see reviews by Saal et al., 2003; Shaham et al., 2000; Sinha, 2007; Stewart, 2003). In male rats, stress can affect responses to morphine-associative learning [reviewed in Bali et al. (2015)]. Latency to drug abuse and relapse due to stressful events are notably higher in females compared to males (Becker, 2017). Importantly, chronic stress results in severe atrophy of CA3 pyramidal cell dendrites and impairs learning processes in male rodents, but not female rodents (Luine et al., 2007; McEwen, 1999; McEwen and Milner, 2007; Sousa et al., 2000). This provides evidence of possible hippocampal involvement in the observed sex differences in addiction-associated learning. However, whether chronic stress impacts these processes differently in females and males is unknown.

Our recent molecular and anatomical studies indicate that chronic immobilization stress (CIS) alters the levels of Leu-Enkephalin (LEnk) and redistributes delta and mu opioid receptors (DORs and MORs, respectively) in the hippocampus in female, but not male rats. The changes in the opioid system in females would promote excitation and essentially “prime” the hippocampus for learning processes following subsequent opioid exposure (Fig. 1). In males, but not females, CIS down-regulates expression of opioid, stress and other signaling molecules in the hippocampus that are important for mediating synaptic plasticity (Randesi et al., 2018). In mossy fiber – CA3 synapses, both mossy fiber LEnk levels and DOR density in CA3 dendritic spines remain elevated in females regardless of estrogen state following CIS (Mazid et al., 2016; Pierce et al., 2014). The increase in DORs in CA3 spines following CIS in females resembles that seen previously in females at high estrogen states

(Harte-Hargrove et al., 2015). In contrast, L_{ENk} levels and DOR density in mossy fiber – CA3 synapses are markedly reduced in CIS males. Moreover, plasmalemmal-associated DORs remain increased in CA3 pyramidal cell dendrites in CIS females but are decreased in CIS males (Mazid et al., 2016). The increased levels of DORs in mossy fiber spine synapses, together with the elevated levels of L_{ENk}s, which have a high affinity for DORs (Corbett et al., 1993) suggest the likelihood for excitation and opioid-dependent LTP at mossy fiber – CA3 synapses in CIS females (Harte-Hargrove et al., 2015; Moore et al., 1994). In addition, other synaptic plasticity processes in distal CA3 dendrites would remain intact in CIS females but would be severely diminished in CIS males.

In the dentate gyrus (DG), CIS further increases plasmalemmal-associated MORs on parvalbumin (PARV)-containing interneuron dendrites in females (Milner et al., 2013). As PARV interneurons synapse on the somata of granule cells (Drake et al., 2007), this rearrangement of the MORs in γ -amino butyric acid (GABA)-ergic interneurons would promote a greater disinhibition, and thus, a relative activation of granule cells in response to an opioid ligand (Drake and Milner, 2006). Moreover, CIS in females mobilizes DORs near the plasmalemma of GABAergic neuropeptide Y/somatostatin (NPY/SOM) interneuron dendrites (Mazid et al., 2016) to granule cell dendrites where they converge with entorhinal afferents (Milner and Bacon, 1989a; Milner and Veznedaroglu, 1992). DORs inhibit NPY release; thus opioid ligand activation of DORs on NPY-containing interneurons would promote lateral perforant pathway LTP (Sperk et al., 2007). In contrast to females, CIS in males does not alter the subcellular distribution of MORs in PARV-labeled interneuron dendrites (Milner et al., 2013) and decreases plasmalemmal associated DORs in GABAergic interneuron dendrites (Mazid et al., 2016). This suggests that CIS essentially “shuts down” these interneuron circuits in males. Thus, as in CA3, CIS rearranges MORs and DORs within two interneuron circuits in the DG of females in a manner that would promote excitation and opioid-associative learning processes.

When subject to a conditioned place preference (CPP) paradigm to the MOR agonist oxycodone, our recent study showed that both unstressed females and males acquire oxycodone CPP and have sex-specific alterations in the opioid system that would facilitate opioid-associative learning processes in females [Fig. 1; Ryan et al. (2018)]. In particular, DORs were redistributed within CA3b pyramidal cell dendrites and in mossy fiber – CA3 synapses in both oxycodone-injected (Oxy) females and males in a manner resembling that shown to be important for opioid-mediated LTP in high estrogen females (Harte-Hargrove et al., 2015; Ryan et al., 2018). However, unlike males, DORs and MORs redistributed in hilar interneurons in Oxy-females in a manner that could enhance disinhibition of granule cells via two different circuits: 1) the number of DOR-labeled cells increased in the hilus; and 2) plasmalemmal-associated MORs and DORs increased in PARV-labeled dendrites and GABAergic interneuron dendrites, respectively (Ryan et al., 2018).

Together, these findings indicate that under unstressed conditions, mechanisms promoting opioid-associative learning processes in the hippocampus are in place in both females and males. However they also suggest that following CIS hippocampal circuits that mediate opioid-associative learning are disrupted in males. The present study examined the effect of CIS on the acquisition of oxycodone CPP as well as alterations in mossy fiber L_{ENk} levels

and the redistribution of DORs and MORS in hippocampal neurons using light and electron microscopic (EM) immunocytochemical methods.

MATERIALS & METHODS

Animals

All procedures were approved by the Rockefeller University and Weill Cornell Medicine Institutional Animal Care and Use Committees, and were in compliance with the 2011 (8th edition) NIH guidelines for the Care and Use of Laboratory Animals. One cohort of adult female (~225–250 grams at the time of arrival) and male (~275–325 grams at the time of arrival) Sprague-Dawley rats (N=24; RGD Cat# 734476, RRID:RGD_734476) was used for this study. Rats were placed in the same room upon arrival and single-housed in R20 rat cages (10.5 in × 19 in × 8 in; Ancare, Bellmore NY) with free access to food (PicoLab Rodent diet 20; LabDiet, St. Louis MO) and water. The cages were placed in custom-built cabinets (Phenome Technologies Inc.) attached directly to the ventilation system and equipped with lamp timers that maintained a 12:12 light/dark cycle (lights on at 0600). Upon arrival to the animal facility, rats were acclimated for one week prior to initiating the experiments. All rats used in this study were first subjected to CIS followed by the CPP behavior; all rat handling, CIS and CPP behavioral testing were conducted between 9:00 am and 1:00 pm each day by the same investigators.

Handling and Estrous Cycle Determination

The rats were picked up and gently stroked for 3–5 minutes per day for five days prior to beginning the CIS procedure, which is known to reduce corticosterone concentrations (Deutsch-Feldman et al., 2015). Prior studies have demonstrated that regular estrous cycle monitoring of rodents using vaginal lavage or swabbing can attenuate associative memory behaviors including cocaine CPP (Van Kempen et al., 2014; Walker et al., 2001; Walker et al., 2002). Moreover, a significant preference for side in the CPP apparatus can be induced by regular estrous cycle monitoring with vaginal lavage alone (Walker et al., 2002). Thus, given these pitfalls combining estrous cycling with CPP behavior as well as the difficulty in mimicking this exact process in males, we determined estrous cycle stage of female rats using vaginal smear cytology (Turner and Bagnara, 1971) only on the terminal day of the experiment after the rats were euthanized.

CIS procedures

CIS procedures were conducted for 10 consecutive days and were identical to those described previously (Mazid et al., 2016). For this, rats were placed in plastic cone shaped polyethylene bags with a small apical hole for their nose and a Kotex mini-pad underneath them for urine collection. The rats were sealed with tape in the bag and left undisturbed for 30 minutes each day. Rats started the CPP training 2 days following the last stress session. Our prior study showed that CIS does not disrupt estrous cycles in female rats (Milner et al., 2013).

Oxycodone CPP procedures

Rats were subjected to oxycodone CPP similar to that described in our recent study (Ryan et al., 2018). Behavioral experiments were staged over a period of 4 days, so that euthanasia for all rats would occur between 9:00 am and 1:00 pm at the termination of the CPP behavior. The CPP apparatus (Med Associates Inc., Fairfax VT) is comprised of three colored compartments (white, black and a central gray) separated by removable doors. Locomotor activity and duration in each compartment were monitored using infrared photobeams. A dose of 3 mg/kg i.p. oxycodone was administered because it has been shown to induce 90–100% CPP in female and male rats in prior studies (Olmstead and Burns, 2005; Ryan et al., 2018). The dose and duration of oxycodone in the present study were much lower than those in oxycodone self-administration studies in Sprague-Dawley rats in which the females had normal estrous cycles (Mavrikaki et al., 2017).

The 14-day CPP protocol had three segments: 1) preconditioning: On day 1, the compartment doors were removed and rats were given free access to the entire apparatus for 30 minutes. As all CIS rats preferred the white compartment, we proceeded using a biased CPP design where oxycodone administration occurred in the less-preferred black compartment (Prus et al., 2009). 2) CPP training: On days 2 through 9, the removable doors were added to separate the black and white compartments and the rats underwent 4 training sessions. On the first day of each session, the rats were injected with oxycodone (3 mg/kg, i.p.) or saline and placed in the black compartment for 30 minutes [a time point within the 3–5 hour half-life of oxycodone (Ordonez Gallego et al., 2007)]. On the second day of each session, the rats were injected with saline and placed in the white compartment for 30 minutes. Control rats were injected with saline prior to placement in either the black or white compartment for 30 minutes. 3) CPP test: On day 14 (4 days following the last injection), the doors separating the compartments were removed. The rats did not receive any injections and were placed in the neutral, central gray compartment of the CPP apparatus and their behavior was monitored for 30 minutes. Percent time in the Oxy-paired compartment was calculated by dividing the time spent in the Oxy-paired chamber over the time spent in both the Oxy- and Saline-paired chambers. Preference score was calculated by subtracting the percent time in the Oxy-paired chamber during the pre-test from that of the post-test.

Immunocytochemistry Procedures

Section Preparation—Euthanasia of all rats was performed by the same investigators and occurred immediately after the completion of the behavioral experiments between 9:00 am and 1:00 pm over a period of 4 days. Rats were deeply anesthetized with ketamine (100 mg/kg) and xylazine (10 mg/kg) and perfused through the ascending aorta sequentially with: 1) 10–15 ml 0.9% saline and 2% heparin, 2) 50 ml of 3.75% acrolein and 2% paraformaldehyde (PFA) in 0.1 M phosphate buffer (PB; pH = 7.4), and 3) 200 ml of 2% PFA in PB. Brains were removed from the skull, cut into 5 mm coronal blocks, and post-fixed in 2% PFA in PB for 30 minutes then transferred into PB. Sections (40 μ m thick) were cut through the hippocampus using a Vibratome (VT1000S, Leica Microsystems, Buffalo Grove, IL) and collected into 24-well plates containing PB. Sections then were placed into a cryoprotectant solution (30% sucrose and 30% ethylene glycol in PB) and stored

at -20°C . For each immunocytochemical experiment, dorsal hippocampal [-3.5 to -4.2 mm from Bregma (Swanson, 1992)] sections were selected. To ensure identical labeling conditions between groups, the sections were coded with hole punches (Pierce et al., 1999) and processed together in single containers. To neutralize reactive aldehydes, sections were incubated in 1% sodium borohydride in PB for 30 minutes (Milner, 2011) then rinsed 8–10 times in PB until gaseous bubbles disappeared.

Antibody Characterization

DOR: This study used a rabbit polyclonal antibody against amino acids 3–17 of DOR protein (Millipore Cat# AB1560, RRID:AB_90778). As described previously (Mazid et al., 2016), this antibody has been extensively characterized in Western blots of lysates from rat brains and in NG108–15 cells, which endogenously express DORs (Barg et al., 1984; Persson et al., 2005; Saland et al., 2005) and in preadsorption controls on tissue sections (Olive et al., 1997). Moreover, immunolabeling for this antibody is not detected in Western blots of COS-7 cells [see Supplemental Fig. 1 in (Williams et al., 2011)], which do not endogenously express DORs (Kieffer et al., 1992) as well as in tissue sections from DOR knockout mice containing the dorsal raphe [Supplemental Fig. 1 (Bie et al., 2010)]. Further, the prominence of DOR-immunoreactivity (-ir) with AB1560 in interneurons compared to pyramidal cells in the rat hippocampus is consistent with DOR mRNA expression (Mansour et al., 1994) as well as DOR binding (Crain et al., 1986; Gulya et al., 1986; Mansour et al., 1987; McLean et al., 1987) in this species. The AB1560 antibody has been used in our previous light and EM studies (Mazid et al., 2016; Ryan et al., 2018). DOR-ir in the rat hippocampus yields the most intense labeling with 3.75% acrolein and 2% PFA fixed sections compared to 4% PFA fixed sections (Commons and Milner, 1997).

LEnk: A mouse monoclonal antibody to LENk from Sera Labs (MAS 083p, clone NOCI, Lot P91G083; Crawley Down, UK) was employed in this study. This antibody recognizes LENk, and to a lesser extent met-enkephalin and dynorphin, but not β -endorphin in immunoblots and adsorption controls (Milner et al., 1989). This antibody has been used previously to immunolabel the rat and mouse hippocampal mossy fiber pathway (Pierce et al., 2014).

GABA: A rat polyclonal antiserum selective against GABA-glutaraldehyde-hemocyanin conjugates was provided courtesy of Dr. Andrew Towle (formerly at Cornell University Medical College). Immunoreactivity for this antibody is abolished following preadsorption with GABA-bovine serum albumin (BSA), but not unconjugated GABA or BSA conjugated to glutamate, β -alanine or taurine (Lauder et al., 1986). Immunolabeling of this antiserum is consistent with that of other GABA-specific antisera (Lauder et al., 1986). This antibody has been used in previous light and EM studies (Drake and Milner, 1999; Mazid et al., 2016).

MOR: A rabbit polyclonal antibody (Neuromics Cat# RA10104–150, RRID:AB_2156526) was used in this study. The antibody specifically recognizes a 15-amino acid sequence (residues 384–398) in the C-terminus of MOR1, but does not recognize the spliced variant MOR-1B-E or the cloned DOR (Abbadie et al., 2000; Arvidsson et al., 1995). The specificity of this antibody has been demonstrated through Western blotting, adsorption

controls, and omission controls in rat tissue (Arvidsson et al., 1995; Drake and Milner, 1999). The predominance of MOR-ir in PARV-labeled dendrites that we see in this study and in our previous studies (Milner et al., 2013; Torres-Reveron et al., 2009a) is corroborated by studies showing elevated MOR mRNA expression within subsets of GABAergic cells in the hippocampus (Stumm et al., 2004). Our previous study revealed that MOR- and PARV-ir are most commonly co-localized, while MOR and SOM, another subset of GABA cells, are less likely to be co-localized (Drake and Milner, 2006).

PARV: A mouse monoclonal PARV antibody (Sigma-Aldrich Cat#P3088, RRID:AB_477329) was used in this study. This antibody has been previously identified by its ability to recognize PARV in brain tissue by immunoblots and radioimmunoassay (Celio, 1990; Celio et al., 1988).

Light Microscopic Immunocytochemistry

Experimental procedure: To investigate changes in the density of LENk-ir and DOR-ir in hippocampal tissue, sections were processed using previously described methods (Milner, 2011). Briefly, tissue sections were rinsed in 0.1 M Tris-buffered saline (TS; pH = 7.6) and blocked in 0.5% BSA in TS for 30 minutes prior to incubation in either mouse anti-LENk (1:15,000) or rabbit anti-DOR antibody (1:5000) in 0.1% BSA and TS for 24 hours at room temperature (25°C) followed by an additional 24 hour incubation at 4°C. Triton X-100 (0.25%) was added to the LENk antibody diluent. Sections were then incubated in a 1:400 dilution of either biotinylated horse anti-mouse immunoglobulin (IgG; LENk; Vector Laboratories Cat# BA-2001; RRID:AB_2336180) or donkey-anti-rabbit IgG (DOR; Jackson Immunoresearch Laboratories, Cat# 711-506-152, RRID:AB_2616595) for 30 minutes and rinsed in TS. Next, sections were incubated in avidin-biotin complex (ABC; Vectastain elite kit, Vector Laboratories, Burlingame, CA) at half the manufacturer's recommended dilution for 30 minutes, washed in TS, and reacted in 3,3'-diaminobenzidine (DAB; Sigma-Aldrich, St. Louis, MO) in 3% H₂O₂ in TS for 10 minutes (LENk) or 3.5 minutes (DOR). Sections were rinsed in TS between each step. Tissue sections then were mounted from 0.5 M PB on 1% gelatin-coated glass slides, dehydrated through an ascending series of ethanol concentrations, and coverslipped from xylene using DPX mounting media (Sigma-Aldrich).

Analysis 1:

LENk and DOR levels: This analysis as well as those described in subsequent sections were performed by a person blinded to experimental conditions. Densitometric quantification for LENk-ir and DOR-ir within the hippocampus was performed using previously described methods (Pierce et al., 2014; Williams and Milner, 2011; Williams et al., 2011). Briefly, images of the hippocampus were captured at 2x (except for LENk-ir in stratum oriens which was captured at 10x) on a Nikon Eclipse 80i microscope using a Micropublisher 5.0 digital camera (Q-imaging, BC, Canada) and IP Lab software (Scanalytics IPLab, RRID:SCR_002775). Average pixel density within regions of interest (ROI) was determined using ImageJ64 (ImageJ, RRID:SCR_003070) software. For LENk, seven ROIs within the hippocampus were selected: the crest, central region, and dorsal blade of the DG, stratum lucidum (SLu) of CA3a, b and c and stratum oriens (SO) lateral to CA3a. For DOR, SO, SLu and stratum radiatum (SR) of CA3b were measured. To control for

variations in overall illumination levels between images and to compensate for background staining, the pixel density of a small region lacking labeling (LEnk: CA1 SR; DOR: corpus callosum) was subtracted from ROI measurements. The accuracy of this technique has been corroborated by a strong linear correlation between average pixel density and actual transmittance (Pierce et al., 2014).

Analysis 2: DOR cell counts: To determine the number of DOR cells in the hilus of the DG, previously described methods were used (Mazid et al., 2016). All DOR-labeled cells containing a nucleus within the hilus of the DG were counted. The area of the hilus was then measured with ImageJ64 software using the granule cell layer and CA3 pyramidal cell layer as borders, and the number of cells per mm² was then calculated. The number of cells in the crest, central hilus and dorsal blade of the hilus was determined by randomly placing a 200 μm² rectangle over these regions using the granule cell layer as a guide.

Dual Labeling Electron Microscopic Immunocytochemistry

Experimental procedure: Tissue sections were dual labeled for either MOR and PARV or DOR and GABA as previously described (Mazid et al., 2016; Milner et al., 2013). Briefly, tissue sections were rinsed in TS and blocked in 0.5% BSA in TS for 30 minutes and then placed in a cocktail of the primary antibodies in 0.1% BSA in TS: MOR (1:1000) + PARV (1:3000) or DOR (1:5000) + GABA (1:1000). Sections were placed on a shaker at room temperature for 24 hours followed by four days at 4°C (145 RPM). Next, sections were processed for peroxidase labeling as described above except that either horse anti-mouse IgG (PARV; Vector Laboratories Cat# BA-2001; RRID:AB_2336180) or biotinylated donkey anti-rat IgG (GABA; Jackson Immunoresearch Laboratories, Cat# 712-065-150, RRID:AB_2340646) was used as a secondary antibody. Sections were placed in DAB in 3% H₂O₂ in TS for 7 minutes (PARV) or 14 minutes (GABA). Sections were washed in TS and incubated in donkey anti-rabbit IgG (DOR and MOR) conjugated to 1 nm gold particles [diluted 1:50; Electron Microscopy Sciences (EMS) Cat# 810.311, RRID:AB_2629850] in 0.01% gelation and 0.08% BSA dissolved in 0.01 M phosphate-buffered saline (PBS) at 4°C overnight. Tissue sections then were rinsed in PBS, postfixed in 2% glutaraldehyde (in PBS) for 10 minutes, and then rinsed in PBS followed by 0.2 M sodium citrate buffer (pH = 7.4). IgG conjugated gold particles were enhanced for 6 minutes with silver solution (SEKL15 Silver enhancement kit, Prod No. 15718 Ted Pella Inc.).

Tissue sections next were fixed in 2% osmium tetroxide for 1 hour, washed in PB and dehydrated in ascending concentrations of ethanols and propylene oxide then embedded in EMbed 812 (EMS, #14120). Ultrathin hippocampal tissue sections (approximately 70–72 nm thick) were cut from ROIs and collected on 400 mesh thin-bar copper grids (EMS, T400-Cu), followed by counterstaining with uranyl acetate (EMS, #22400) and Reynolds lead citrate (lead nitrate EMS, #17900–25). In CA3, samples contained SO, PCL, SLu and SR. In the DG, samples primarily contained the crest and central hilus.

Identification of EM profiles: Tissue sections containing ROIs were examined on a Tecnai Biotwin transmission electron microscope (FEI, Hillsboro, OR). Images were captured at a magnification of 13500x and profiles were classified as neuronal or glial based on standard

morphology (Peters, 1991). Dendrites contained microtubules and mitochondria and were post-synaptic to axon terminals. Dendrites were classified as large (diameter > 1.0 μm) or small (diameter < 1.0 μm). Axon terminals were identified by the presence of numerous small synaptic vesicles. Mossy fiber terminals were large (1 – 2 μm in diameter) and often contacted multiple dendritic spines of CA3 pyramidal cells (Pierce et al., 2014). Immunoperoxidase was identified as an electron-dense precipitate within PARV- or GABA-containing dendrites, and silver intensified immunogold (SIG) labeling for MOR and DOR was identified as black electron-dense particles (Milner, 2011).

Analysis 1: dendritic profiles.: Micrographs containing SIG labeled dendrites were collected from SR of CA3 and the hilus of the DG as previously described (Mazid et al., 2016). Briefly, 50 randomly selected single labeled dendrites (DOR in CA3b SR) or dual labeled dendrites (MOR/PARV or DOR/GABA in the hilus of the DG) were photographed, and the subcellular localization of DOR-SIG or MOR-SIG particles was determined. Microcomputer Imaging Device software (MCID Analysis, RRID:SCR_014278) was used to assess perimeter, cross-sectional area and diameter, and major and minor axis lengths for each SIG labeled dendrite.

The distribution of MOR-SIG or DOR-SIG particles was analyzed using the following parameters: 1) the number of SIG particles localized to the plasma membrane of the dendrite (PM: μm), 2) the number of SIG particles localized within 50 nm of the plasma membrane (Near PM: μm), 3) the number of SIG particles localized to the cytoplasm per cross-sectional area (CY: μm^2), and 4) the total number of SIG particles per cross-sectional area (Total: μm^2). The partitioning ratio was calculated as the proportion of SIG particles in a given subcellular compartment (on PM, near PM, or in the cytoplasm) divided by the total number of MOR-SIG or DOR-SIG particles within the dendrite.

SIG labeling on the plasma membrane identifies receptor-binding sites whereas SIG labeling near the plasma membrane identifies a pool from which receptors can be added or removed from the plasma membrane (Boudin et al., 1998). SIG labeling in the cytoplasm identifies receptors that are either stored during transfer to or from the soma or another cellular compartment, or the receptors are being degraded or recycled (Fernandez-Monreal et al., 2012; Pierce et al., 2009). When stimulated by an agonist, the ratio of receptors on the plasma membrane to those in the cytoplasm declines, as demonstrated by the number of SIG labeled receptors in each compartment (Haberstock-Debic et al., 2003).

Analysis 2: DOR-labeled dendritic spines contacted by mossy fibers.: The number of DOR-SIG labeled dendritic spines contacted by mossy fibers in SLu of CA3 was determined as previously described (Harte-Hargrove et al., 2015; Mazid et al., 2016; Pierce et al., 2014). For this, 50 randomly selected mossy fibers contacting dendritic spines from the tissue-plastic interface were photographed. The percentage of labeled spines (i.e., spines containing one or more SIG particles) was tallied and then subcellular location of the SIG particle at the synapse, on the plasma membrane or in the cytoplasm was noted.

Analysis 3: DOR-labeled dendritic spines in CA3 SR.: From the SR CA3 micrographs (same as those collected in Analysis 1), 100 spine profiles per rat were randomly identified.

Dendritic spines were included if contacted by a terminal forming an asymmetric synapse and categorized as unlabeled or labeled (with at least one DOR-SIG particle). DOR-SIG particles within spines were classified as in the synapse, on the plasma membrane, or in the cytoplasm.

Analysis 4: number of MOR/PARV cells in DG.: Using the granule cell layer as a guide, the number of soma dually labeled for MOR and PARV in the dorsal blade of the hilus was determined at 4200x. All dually labeled cells containing a nucleus were counted and divided by the number of squares (each 55 μm wide) to determine the number of MOR/PARV cells/ mm^2 .

Figure Preparation

No feature within an image was obscured, moved, removed, introduced or enhanced. Adjustments to brightness, sharpness and contrast were applied uniformly to the image. For light microscope images, the adjustments were made in Microsoft PowerPoint 2010 and were identical to those images from the same experiment. Electron micrographs were increased in resolution (400 dpi) and then adjusted for brightness, sharpness and contrast in Adobe Photoshop 9.0 (RRID:SCR_014199) prior to importing them into Microsoft PowerPoint 2010, where additional adjustments to sharpness, brightness, and contrast were made. These latter adjustments were made to achieve uniformity in appearance between electron micrographs. Graphs were generated using Prism 7 software (Graphpad Prism, RRID:SCR_002798).

Statistical Analysis

Data are expressed as mean \pm SEM. Significant test statistics were set to an alpha < 0.05 . Unless noted, all statistical analyses were conducted on JMP 12 Pro software (JMP, RRID:SCR_014242). CPP data was analyzed using a two-way analysis of variance (ANOVA). For this, the percent change in the preference for the oxycodone-paired box vs. the saline-paired box between the pre- and post-test groups was compared. Locomotor activity was analyzed using a two-way ANOVA (condition \times sex) with repeated measures by conditioning session (oxycodone-injection; days 1, 3, 5, and 7 of paradigm) on Prism 7.

Methods for quantitative densitometric analysis of immunoperoxidase reaction product at the light microscopic level are well established and used in numerous studies (Mazid et al., 2016; Pierce et al., 2014; Pierce et al., 1999; Williams et al., 2011). Optical density sample comparisons between Sal-CIS females and Sal-CIS males, Sal-CIS females and Oxy-CIS females or Sal-CIS males and Oxy-CIS males were determined through one-way ANOVA or Welch t-test ANOVAs for samples with unequal variances (as determined by Levene's test). The numbers of DOR-labeled or MOR/PARV-labeled cells were analyzed using a Student's t-test comparing Sal-CIS females and Sal-CIS males, Sal-CIS females and Oxy-CIS females or Sal-CIS males and Oxy-CIS males.

Quantitative dual labeling EM methods are designed to determine relative changes in the subcellular distribution of proteins in dendrites of different sizes following experimental manipulations. For this, protein distribution of DORs or MORs in dendritic profiles of

different sizes, rather than number of cells or dendrites per animal, is analyzed. To account for errors related to spatial location, only samples from a single plane are analyzed within a section. In these studies, we correct for any size-related differences in dendritic profiles by determining SIG particle density for each dendritic compartment divided by the perimeter (PM/ μm or Near PM/ μm) or cross-sectional area (CY/ μm^2 or Total/ μm^2). To analyze the partitioning ratio of SIG particles within a dendrite, we divided the number of SIG particles in each compartment by the total number of SIG particles in the dendrite (e.g., PM/total).

The number of dendritic profiles per block to be analyzed in quantitative EM studies was determined from our initial studies in which we randomly sampled profiles from 9632 μm^2 of tissue (Znamensky et al., 2003). In these analyses, 50 dendrites on average were sufficient to make quantitative comparisons on the subcellular distribution of proteins. In this study, increasing the number of dendrites to 75 or greater did not change the significance of the results. Within-group comparisons of DOR-SIG distributions in the Sal-CIS female and Sal-CIS male rats were determined through one-way ANOVAs, or Welch t-test ANOVAs for samples with unequal variances (as determined by Levene's test). Comparisons between sex and treatment were analyzed for main effects of sex and treatment (saline vs. oxycodone) with two-way ANOVAs, using Tukey's HSD post-hoc analyses for specific between-group differences. Analysis of DOR-SIG labeling in MF – CA3 synapses was done using two-way ANOVAs, followed by Tukey's HSD post-hoc analyses.

RESULTS

Females, but not males, acquire oxycodone CPP following CIS

Two-way ANOVA showed a significant main effect of condition (saline vs. oxycodone CPP) [$F(3,19) = 10.6507$, $p = 0.0041$]. There was no significant main effect of sex or a significant interaction between sex and condition. Post-hoc analysis revealed that CIS female rats had a significant increase in the percent change in preference score for the oxycodone-associated compartment ($p = 0.0147$) while the CIS male rats did not (Fig. 2). On testing day, saline-injected (Sal) rats from both sexes showed no preference for either compartment. There were no significant differences in locomotion in CIS female or male rats in the four training sessions when they were injected with saline or oxycodone (Supplemental Table 1). On the day of euthanasia, all CIS female rats were in the estrus phase of the estrous cycle.

LEnk levels are modestly reduced in Oxy-CIS females compared to Sal-CIS females

Consistent with our previous studies (Pierce et al., 2014; Torres-Reveron et al., 2008), LEnk-ir is diffusely distributed in the hilus of the DG and in SLu of CA3 (i.e., the mossy fiber pathway; Fig. 3A). However, there were no differences in the optical density of LEnk-ir either in CA3 or the DG between Sal-CIS females and Sal-CIS males (Fig. 3C,D). Oxy-CIS females compared to Sal-CIS females showed a significant decrease in the optical density of LEnk-ir in SLu of CA3c ($F_{1,9} = 5.1484$; $p = 0.0494$; Fig. 3B,C) and a trend for a decrease in the optical density of LEnk-ir in CA3a ($F_{1,9} = 4.2673$; $p = 0.0688$). However, there were no differences in the densities of LEnk-ir in any mossy fiber subregion between Sal-CIS and Oxy-CIS males (Fig. 3C,D).

Many types of experimental manipulations can induce mossy fiber sprouting into CA3 SO [reviewed in Scharfman and MacLusky (2014)]. Our previous study showed sprouting of LENk-labeled fibers into CA2/CA3a in unstressed Oxy females (Ryan et al., 2018). In the present study, no significant differences were found in the LENk labeling in CA3 SO in any cohort of CIS rats (not shown).

DOR levels in CA3b are similar in all groups of CIS females and males

Previously, we demonstrated that CIS altered the optical density of DOR-ir in CA3 SR such that no differences were detectable between female rats from different estrous cycle stages or males (Mazid et al., 2016). Moreover, we recently found that Oxy-CPP in unstressed rats did not alter the optical density of DOR-ir in SO, SLu or SR of CA3 in either females or males (Ryan et al., 2018). As in previous studies, diffuse DOR-ir was found throughout the layers of CA3 but was densest in SLu (Fig. 4A). There were no significant differences in the optical density of DOR-ir in SO, SLu or SR of CA3 between any of the CIS group (Fig. 4B).

Oxycodone CPP alters the densities of DORs in CA3 dendrites in Oxy-CIS females

Representative micrographs showing DOR-SIG labeling in CA3 pyramidal cell dendrites in SR for all four groups are shown in Figure 4C–F. These dendrites often had spines, many of which were contacted by terminals forming asymmetric synapses (examples in Fig. 4C,D). Compared to Sal-CIS males, Sal-CIS females had a significantly lower density of DOR-SIG particles in the cytoplasm ($F_{1,254} = 5.0146$; $p = 0.0260$; Fig. 5C) and in total ($F_{1,255} = 7.2207$; $p = 0.0077$; Fig. 5D) in CA3 dendrites with no differences in partitioning ratio. When the dendrites were separated into large ($> 1\mu\text{m}$) and small ($< 1\mu\text{m}$), there were no significant differences between Sal-CIS females and males (not shown).

Two-way ANOVA showed a significant main effect of sex on the total density of DOR-SIG particles ($F_{3,596} = 4.4556$; $p = 0.0352$) in CA3 pyramidal cell dendrites. The sex by treatment interaction was significant among cytoplasmic density ($F_{3,596} = 3.9095$; $p = 0.0485$) of DOR-SIG particles in CA3 dendrites. When CA3 DOR-labeled dendrites were further divided into large and small dendrites, the sex by treatment interaction was significant among cytoplasmic density ($F_{3,242} = 5.9984$; $p = 0.0150$) of DOR-SIG particles in small dendrites in CA3. There were no significant ANOVA results for partitioning ratios of total dendrites. When divided into large and small dendrites, however, there was a significant sex by treatment interaction in the ratio of near plasma membrane DOR-SIG particles in large CA3 dendrites ($F_{3,350} = 4.7359$; $p = 0.0302$) and in the ratio of cytoplasmic DOR-SIG particles in small CA3 dendrites ($F_{3,242} = 4.0081$; $p = 0.0464$).

Post-hoc analysis revealed that no significant differences in the density of DOR-SIG particles in CA3 dendrites in Oxy-CIS females or males were seen (Fig. 5A–D). In summary, these results demonstrate that Sal-CIS males have higher densities of cytoplasmic DORs in CA3 pyramidal cell dendrites than Sal-CIS females. However, following oxycodone CPP, DORs redistribute to be comparable between Oxy-CIS females and males.

DOR-labeling in mossy fiber – CA3 synapses is elevated in females compared to males

Consistent with previous studies (Harte-Hargrove et al., 2015; Mazid et al., 2016), DOR-SIG particles were found in mossy fiber - CA3 synapses (example Fig. 6A). Two-way ANOVA showed a significant main effect of sex on the percentage of DOR-labeled mossy fiber – CA3 synapses ($F_{3,8} = 15.0193$; $p = 0.0047$) as well as on the number of DORs located in the cytoplasmic compartment of mossy fiber - CA3 synapses ($F_{3,8} = 14.5349$; $p = 0.0051$).

Post-hoc analysis revealed a significant increase in the percentage of DOR-labeled CA3 dendritic spines contacted by mossy fibers in Oxy-CIS females compared to Oxy-CIS males ($p = 0.0334$; Table 1). When divided by compartment, there was an increase in the number of cytoplasmic DOR-labeled spines contacted by mossy fibers in CA3 in Oxy-CIS females compared to Oxy-CIS males ($p = 0.0478$; Table 1). There was no difference in number or percentage of DOR-labeled spines between Sal-CIS and Oxy-CIS females or Sal-CIS and Oxy-CIS males.

In CA3 SR, DOR-SIG particles were observed in dendritic spines in all four groups (example Fig. 6B). There were no significant differences in the percentage of DOR-labeled dendritic spines between Sal-CIS and Oxy-CIS females or males (Table 1). Qualitatively, Sal-CIS male rats had less DOR-SIG particles in the synapse, on the membrane, and in the cytoplasm of CA3 dendritic spines in SR compared to the three other groups (Table 1).

In summary, Oxy CPP in the CIS females is accompanied by an increase in DORs at the mossy fiber – CA3 synapse. This elevation in DORs is not seen in the Oxy-CIS males who notably do not acquire CPP.

The number of DOR hilar interneurons is similar in Sal- and Oxy-CIS females and males

Our previous studies showed that CIS increases the number of DOR-labeled neurons in the dorsal blade of the DG in females but not males (Mazid et al., 2016). Consistent with these studies, DOR-labeled neurons were primarily found in the crest, central and dorsal blade of the hilus of the DG (Fig. 7A–C). However, in contrast to prior studies, there were no significant differences in the total number of DOR-labeled hilar neurons among the four groups (Table 2). Moreover, there were no significant differences in the number of DOR-labeled neurons in any of the subregions (crest, central or dorsal blade) among any of the four groups.

The density of DORs in hilar GABAergic dendrites is elevated in CIS females

Photomicrographs showing DOR-SIG labeling in GABA-labeled hilar dendrites are shown for all four groups in Figure 7D–G. In both CIS females and males, numerous terminals forming asymmetric synapses contacted the dual labeled dendrites (examples in Fig. 7D–G). Two-way ANOVA showed a significant main effect of sex in DOR-SIG total ($F_{3,343} = 12.6627$; $p = 0.0004$) and cytoplasmic density ($F_{3,343} = 5.2755$; $p = 0.0222$) in large GABA-labeled dendrites. In small GABA-labeled dendrites, a significant main effect of sex also was seen in total density of DOR-SIGs ($F_{3,249} = 47.0934$; $p < 0.0001$) as well as the density of DOR-SIGs on the plasma membrane ($F_{3,249} = 4.7000$; $p = 0.0311$), near the

plasma membrane ($F_{3,249} = 4.0057$; $p = 0.0464$), and in the cytoplasm ($F_{3,249} = 4.5106$; $p = 0.0347$).

Post-hoc analysis revealed no significant differences in the density or partitioning ratio of DORs in GABA dendrites in CIS females or males (not shown). However, when dendrites were separated by size, Sal-CIS females had a greater density of cytoplasmic ($F_{1,145} = 7.0414$; $p = 0.0089$; Fig. 8C) and total ($F_{1,172} = 6.3258$; $p = 0.0128$; Fig. 8D) DOR-SIG particles than Sal-CIS males in large dendrites, and a greater density of total ($F_{1,124} = 17.5051$; $p < 0.0001$) DOR-SIG particles in small dendrites (not shown). Oxy-CIS females had a greater total DOR-SIG particle density than Oxy-CIS males in large ($p = 0.0318$; Fig. 8D) and small ($p < 0.0001$; not shown) hilar GABA dendrites. There were no significant differences in density of DORs in other compartments in small GABA dendrites in any of the groups. Moreover, there were no significant differences in the partitioning ratio of DORs in GABA dendrites in any compartments or in total between Sal-CIS and Oxy-CIS females or males (not shown).

MORs differentially redistribute in PARV dendrites in CIS females and males

In the hilus of the DG, PARV-labeled cells are primarily found in the subgranular zone (Fig. 9A). Consistent with our previous studies (Milner et al., 2013; Torres-Reveron et al., 2009b), MOR-SIG labeling was co-localized with PARV in soma and dendrites (Fig. 9B). By electron microscopy, there were no significant differences in the number of MOR/PARV somata per mm^2 in the dorsal blade of the hilus in Sal-CIS female and male rats. However, Oxy-CIS females had fewer MOR/PARV cells per mm^2 in the dorsal blade of the hilus compared to Sal-CIS females (Sal-CIS female: 0.51 ± 0.05 cells per 100 microns; Oxy-CIS female: 0.32 ± 0.02 cells per 100 microns; $t_5 = 3.16$; $p = 0.0343$). No difference was observed in the number of MOR/PARV cells between Sal-CIS and Oxy-CIS males.

Representative micrographs of dendrites dually labeled for MOR-SIG and PARV-immunoperoxidase from each experimental group are presented in Figure 9C–F. In both CIS females and males, numerous terminals formed asymmetric synapses on the MOR/PARV-labeled dendrites. Two-way ANOVA revealed significant main effects of treatment (saline vs. oxycodone) in MOR-SIG density in PARV dendrites on the plasma membrane ($F_{3,596} = 5.8842$; $p = 0.0156$) and a main effect of sex on total ($F_{3,596} = 8.5267$; $p = 0.0036$) and cytoplasmic ($F_{3,596} = 4.8721$; $p = 0.0277$) MOR-SIG density in PARV dendrites. Sex by treatment interaction was not significant for MOR-SIG densities in PARV dendrites. MOR/PARV-labeled dendrites were then separated into large (i.e., proximal) and small (i.e., distal), and analyzed. In large dendrites, there was a main effect of treatment in MOR-SIG density in PARV dendrites in total ($F_{3,495} = 10.764$; $p = 0.0011$) and on the plasma membrane ($F_{3,495} = 5.964$; $p = 0.0149$) and a main effect of sex in total ($F_{3,495} = 5.8885$; $p = 0.0156$) and cytoplasmic ($F_{3,495} = 3.8708$; $p = 0.0497$) MOR-SIG density in PARV dendrites. In small dendrites, there was a significant sex by treatment interaction of MOR-SIG density in PARV dendrites near the plasma membrane ($F_{3,97} = 4.3799$; $p = 0.0390$) only.

Post-hoc analyses demonstrated that Oxy-CIS females had a greater total density of MOR-SIG particles in PARV dendrites compared to Oxy-CIS males ($p = 0.0422$; Fig. 10D). When separated based on size, Oxy-CIS males had a significantly greater density of MOR-SIG

particles on the plasma membrane of large PARV dendrites compared to Sal-CIS males ($p = 0.0083$; Fig. 10A). Additionally, Oxy-CIS females had a greater density of MOR-SIG particles in the cytoplasm in large PARV dendrites compared to Oxy-CIS males ($p = 0.0321$; Fig. 10C). There were no significant differences in the partitioning ratio of MORs in large or small PARV dendrites between Sal-CIS and Oxy-CIS females or males (not shown).

DISCUSSION

The results of this study demonstrate that CIS females, but not males, acquire oxycodone CPP and that CIS redistributes DORs and MORs within hippocampal CA3 pyramidal cells and interneurons in females, but not males. These results suggest mechanisms for promoting excitation and essentially “priming” the hippocampus for opioid-associated learning in CIS females and “shutting down” key synapses necessary for opioid-associative learning in CIS males (Fig. 11). In particular, Sal- and Oxy-CIS females, but neither group of CIS males, had elevated DOR densities in mossy fiber – CA3 dendritic spines, which we have previously shown are important for opioid-mediated LTP (Harte-Hargrove et al., 2015). In the DG, Sal- and Oxy-CIS females compared to both groups of CIS males had elevated levels of DORs and MORs in GABAergic interneuron dendrites, suggesting capacity for greater synthesis or storage of these receptors in circuits important for opioid-mediated disinhibition. It is possible that low levels of DORs in mossy fiber – CA3 synapses and hilar GABAergic interneurons may contribute to the attenuation of oxycodone CPP in males exposed to CIS.

Methodological Considerations

The present manuscript is part of a continuum of studies that we have performed over the last decade aimed at understanding sex differences in the hippocampal opioid system in relation to drug-related learning in unstressed and stressed conditions (Mazid et al., 2016; McEwen and Milner, 2017; Randesi et al., 2018). We designed the present study based on our collective experiences as well as knowledge of the literature regarding estrous cycling, stress and opioids. To achieve rigorous and reproducible results in this study, we aimed to minimize interfering processes that could skew the CPP behaviors, e.g., monitoring estrous cycling and hormone replacement (Van Kempen et al., 2014; Walker et al., 2001; Walker et al., 2002). In addition, the present experiments were performed on a single cohort of female and male animals that underwent CIS and subsequent CPP behavior at the same time. In this cohort, the female rats were in estrus at the termination of the experiment. Moreover, to control for variability in immunocytochemical processing and reagents, the quantitative light and EM immunocytochemical studies were processed in one experiment. Estrous cycle phase can influence LEnk levels and the subcellular distribution of DORs and MORs in hippocampal neurons (McEwen and Milner, 2017). Thus, a future study is necessary to elucidate estrous cycle effects on the hippocampal opioid system after CIS and Oxy-CPP.

CIS alters acquisition of oxycodone CPP in males but not females

Similar to our previous study of CPP to oxycodone in unstressed rats (Ryan et al., 2018), the CIS rats in this study showed a pre-test side preference in the CPP apparatus. However, unstressed females preferred the black side and unstressed males preferred the white side

whereas both CIS females and males preferred the white side. Notably, both unstressed female and male rats acquired oxycodone CPP (Ryan et al., 2018) whereas the present study demonstrated that only CIS females acquired CPP to oxycodone. CIS also induces dendritic retraction of CA3 pyramidal cells and loss of PARV-labeled interneurons in males but not females [reviewed in McEwen (1999)]. Thus, this could have contributed to the behavioral and anatomical sex differences observed in the present study.

The change in pre-test side preference of the CPP chamber from black to white of the unstressed and CIS females could be due to the increased handling of the CIS cohort or a result of different experimenters performing the studies. Alternatively, the change in side preference in the CPP apparatus could reflect reduction of anxiety or fear in the CIS females. In support, CIS impairs fear extinction in males but facilitates fear extinction in females (Baran et al., 2009). Our observation that CIS males do not acquire CPP to oxycodone is consistent with numerous studies demonstrating that male rodents display impaired cognitive performance after chronic stress (Becker, 2017; Conrad et al., 1996; Kitraki et al., 2004; Luine et al., 2007). This is also in agreement with studies showing decreased CPP scores to morphine following acute and subchronic stress in Wistar male rats (Haghighparast et al., 2014) and chronic unpredictable mild stress in male hooded rats compared to controls (Papp et al., 1992). Interestingly, our findings that Sprague-Dawley male rats do not acquire oxycodone CPP contrast studies showing that chronic foot-shock exposure, corticosterone treatment or inescapable stress potentiate morphine CPP in male Sprague-Dawley rats (Li et al., 2007; Rozeske et al., 2009). These differences could be due to the type of chronic stress and/or the differences in the pharmacodynamics and signaling of oxycodone and morphine. For instance, oxycodone and morphine display distinct binding effects and receptor desensitization (Arttamangkul et al., 2008; Bolan et al., 2002; He et al., 2002) and oxycodone can be a partial kappa opioid receptor agonist (Narita et al., 2008; Nielsen et al., 2007).

Oxycodone CPP alters mossy fiber LEnk levels similarly in unstressed and CIS females

Consistent with our previous studies in unstressed rats (Ryan et al., 2018), oxycodone CPP did not alter the levels of LEnk in mossy fibers in CA3b in CIS females. In contrast, CIS males did not show the increase in mossy fiber LEnk levels in CA3b seen in the unstressed males. Within the mossy fibers, LEnk is stored in dense-core vesicles (DCVs) (Pierce et al., 2014; Pierce et al., 1999) and is released at low frequency stimulation (2 Hz) (Han, 2003; Liang et al., 2010; Wong and Moss, 1992) as well as in response to stress (Bruchas et al., 2008). In addition to opioid peptides, mossy fibers contain high levels of phosphorylated MORs in both unstressed males and females (Gonzales et al., 2011) which likely identify the MOR1D splice variant (Abbadie et al., 2000). As opioid agonists have a high binding affinity for MOR1D (Bolan et al., 2004), the present findings suggest a disruption of the mechanisms accompanying MOR-stimulated increases in LEnk in mossy fibers in males following CIS. This may have functional consequences as our previous studies demonstrated that the elevated LEnk levels in mossy fibers, together with the increased DORs in mossy fiber – CA3 spine synapses in high estrogen (proestrus) female rats, are important for the induction of low-frequency opioid-dependent LTP in CA3b pyramidal cells (Harte-Hargrove et al., 2015). Males do not display this low-frequency opioid-dependent LTP in mossy fiber

synapses (Harte-Hargrove et al., 2015). This lack of LEnk increase in response to oxycodone may place the CIS males, compared to unstressed males, at a disadvantage for acquiring LTP at this synapse, thereby contributing to the lack of oxycodone CPP acquisition.

Similar to studies in unstressed females (Ryan et al., 2018), oxycodone CPP in CIS females reduced LEnk levels in CA3a, where the endings of the mossy fiber projection reside (Torres-Reveron et al., 2008). As DCVs are generated in the cell body and are transported to terminals where they are released (Pierce et al., 2014; Pierce et al., 1999; Zupanc, 1996), this reduction may reflect the inability of DCVs to be replenished in CA3a following oxycodone CPP. Alternatively, oxycodone CPP may release LEnk from mossy fibers in CA3a to bind to the enriched population of phosphorylated DORs present in this region (Burstein et al., 2013).

Although the alterations of LEnk in the mossy fiber pathway seen following oxycodone CPP in CIS females is similar to those in unstressed females, sprouting of Enk-containing mossy fibers into SO is not observed in CIS females. This indicates that CIS likely reduces some forms of synaptic plasticity in females (Scharfman and MacLusky, 2014).

CIS positions DORs in CA3 pyramidal cell dendrites in females in a manner that would promote oxycodone CPP

In Sal- and Oxy-CIS females ~8–11% of the CA3 dendritic spines contacted by mossy fibers contain DORs, similar to unstressed female rats (Ryan et al., 2018). In contrast, the number of DOR labeled mossy fiber – CA3 spine synapses is dramatically reduced in Sal- and Oxy-CIS males compare to their unstressed counterparts (~2% compared to 10–12%). The reduction of DORs in mossy fiber – CA3 synapses combined with the lower levels of LEnk in the mossy fibers described above may have important functional consequences. In particular, low frequency DOR-mediated LTP is present only in proestrus (high estrogen) females but not males, and this correlates with ~ 4–5 more DORs in mossy fiber – CA3 synapses in proestrus females compared to males (Harte-Hargrove et al., 2015). Although our prior studies showed that DORs in CA3 spine synapses slightly decrease in females following CIS, they also showed that the number of DORs in CA3 spines doubles 1 hour after an injection of 3 mg/kg (i.p.) oxycodone (Mazid et al., 2016). Together, these findings suggest that the mechanisms for opioid-dependent LTP at mossy fiber – CA3 synapses are still in place in CIS females but not CIS males.

In the present study, Sal-CIS females had lower levels of DORs in CA3 pyramidal cell dendrites compared to CIS males. Although this sex difference following CIS was not seen in our prior study (Mazid et al., 2016), it likely reflects the differences in hormonal state of the females (estrus vs. diestrus, respectively) in the two studies (Williams et al., 2011). Regardless, the present study showed two important sex differences in the redistribution of DORs within CA3 pyramidal cell dendrites following oxycodone injections and CPP training. First, accompanying oxycodone CPP, CIS females had increased cytoplasmic DORs suggesting that increased pools of DORs are available for recruitment to the membrane. Second, no changes in DOR distribution were observed in the CIS males following oxycodone-injections. This latter finding contrasts with that of unstressed males, who, upon acquiring Oxy-CPP, demonstrated a redistribution of DORs from near the plasma

membrane to the cytoplasm of CA3 pyramidal cell dendrites (Ryan et al., 2018). Together, these results suggest that CIS essentially shuts down DOR trafficking in the males but not the females. These results were not totally unexpected as chronic stress results in the retraction of CA3 pyramidal cell dendrites in males but not females (McEwen et al., 2016).

CIS redistributes DORs and MORs within GABAergic interneurons in females in a way that promotes oxycodone CPP

Regardless of treatment, the present study demonstrated that CIS females compared to CIS males had greater cytoplasmic and total densities of DORs in GABA-labeled interneuron dendrites that previous studies have shown colocalize NPY and SOM (Commons and Milner, 1996; Mazid et al., 2016; Williams and Milner, 2011). This suggests that greater pools of DORs in GABAergic interneurons are available to CIS females compared to CIS males. This finding is consistent with the idea that CIS differentially redistributes DORs within GABAergic interneurons in a way that would promote excitation and plasticity processes in females that are necessary for acquiring oxycodone CPP. Specifically, previous studies demonstrated that following CIS, DORs in GABAergic dendrites redistribute near the plasmalemma in females and away from the plasmalemma in males (Mazid et al., 2016). In response to a single injection of oxycodone (3mg/kg, i.p.) in CIS females, DORs traffic from the near plasmalemma to the plasmalemma where they would be available for subsequent binding with opioid agonists. Consequently, in CIS females compared to CIS males, the four hits of oxycodone during the CPP training session would lead to a greater inhibition of NPY/SOM containing interneurons which project to distal granule cell dendrites where they converge with entorhinal afferents (Milner and Bacon, 1989b; Milner and Veznedaroglu, 1992). Activation of DORs thus would inhibit NPY release from these interneurons, promoting lateral perforant pathway LTP (Sperk et al., 2007).

Although the distribution of MORs within PARV interneuron dendrites was similar in Sal-CIS females and males, MORs redistributed differentially in PARV dendrites in the female and male CIS rats injected with oxycodone. Cytoplasmic and total MORs were increased in PARV dendrites in Oxy-CIS females, suggesting that increased pools of MORs are synthesized and/or transported to the PARV dendrites. Interestingly, MORs were elevated on the plasmalemma of PARV dendrites in Oxy-CIS males compared to Sal-CIS males. Thus, in both CIS females and CIS males, exposure to oxycodone during the CPP paradigm results in a redistribution of MORs within PARV neurons that could enhance disinhibition of granule cell soma in response to opioids either indirectly (females) or directly (males). However, as the synapses between granule cell mossy fibers and DOR-containing CA3 pyramidal cells have reduced function in males, the redistribution of MORs in PARV interneurons would likely have little effect on the network properties of the opioid system.

Functional considerations

The role of gender in processes leading to opioid addiction has been difficult to unravel. In humans, it is challenging to parse out biological effects from genetics, history of self-administration of drugs, multi-drug use and environmental influences. However, our studies in rats have begun to elucidate potential mechanisms that contribute to sex differences in the pathway to opioid addiction. Our studies in unstressed rats demonstrate that although

oxycodone-associative learning occurs in both sexes, MORs and DORs in hippocampal GABAergic interneurons redistribute in a manner that potentially enhances plasticity processes to a greater extent in females. The present studies expand on these findings by revealing that following CIS, females, but not males, acquired oxycodone CPP. Moreover, they show that the mechanisms for promoting opioid-associative learning are in place in three hippocampal circuits in CIS females: 1) granule cell mossy fiber – CA3 pyramidal cell synapses; 2) NPY/SOM-containing interneuron connections with lateral perforant path inputs on the distal dendrites of granule cells; and 3) GABAergic basket cell connections with granule cell somata. Conversely, we find that these same circuits are likely disrupted in CIS males. Though this would be desirable relative to addictive processes, a reduced ability to respond to the endogenous opioids would be disadvantageous under normal conditions. The strengthening of opioid circuits may provide a behavioral or evolutionary advantage to female rodents, allowing them to adjust their performance capacity to hippocampal-dependent associative learning, especially in response to chronic stress. However, the presence of such mechanisms that enhance synaptic plasticity to endogenous opioids could also contribute to the greater susceptibility of female rodents to opioid addiction acquisition and reinstatement (Becker, 2017), especially after chronic stress.

Supplementary Material

Refer to Web version on PubMed Central for supplementary material.

Acknowledgements

Supported by NIH grants DA08259 (T.A.M., M.J.K., B.S.M.), HL098351 (T.A.M.), HL 136520 (T.A.M.), MH041256 (B.S.M.) and MH102065 (J.D.G.), and Hope for Depression Research grant (B.S.M.). We thank Mr. Konrad T. Ben, Ms. June Chan and Dr. Diane Lane for technical assistance.

ABBREVIATIONS

ABC	avidin-biotin complex
BSA	bovine serum albumin
CIS	chronic immobilization stress
CPP	conditioned place preference
DAB	diaminobenzidine
DCV	dense-core vesicle
DG	dentate gyrus
DOR	delta opioid receptor
GABA	Gamma-amino butyric acid
EM	electron microscopic
LEnk	Leu-Enkephalin

LTP	long-term potentiation
MOR	mu opioid receptor
N	nucleus
NPY	neuropeptide Y
Oxy	oxycodone-injected
PARV	parvalbumin
PFA	paraformaldehyde
PB	phosphate buffer
PBS	phosphate-buffered saline
ROI	region of interest
Sal	saline-injected
SIG	silver-intensified immunogold
SLu	stratum lucidum
SO	stratum oriens
SOM	somatostatin
SR	stratum radiatum
TS	tris-buffered saline

References

- Abbadie C, Pan Y, Drake CT, Pasternak GW. 2000. Comparative immunohistochemical distributions of carboxy terminus epitopes from the mu-opioid receptor splice variants MOR-1D, MOR-1 and MOR-1C in the mouse and rat CNS. *Neuroscience* 100(1):141–153. [PubMed: 10996465]
- Arttamangkul S, Quillinan N, Low MJ, von Zastrow M, Pintar J, Williams JT. 2008. Differential activation and trafficking of micro-opioid receptors in brain slices. *Molecular pharmacology* 74(4):972–979. [PubMed: 18612077]
- Arvidsson U, Riedl M, Chakrabarti S, Lee JH, Nakano AH, Dado RJ, Loh HH, Law PY, Wessendorf MW, Elde R. 1995. Distribution and targeting of a mu-opioid receptor (MOR1) in brain and spinal cord. *The Journal of Neuroscience: The Official Journal of the Society for Neuroscience* 15(5 Pt 1):3328–3341.
- Bali A, Randhawa PK, Jaggi AS. 2015. Stress and opioids: role of opioids in modulating stress-related behavior and effect of stress on morphine conditioned place preference. *Neuroscience and Biobehavioral Reviews* 51:138–150. [PubMed: 25636946]
- Baran SE, Armstrong CE, Niren DC, Hanna JJ, Conrad CD. 2009. Chronic stress and sex differences on the recall of fear conditioning and extinction. *Neurobiology of Learning and Memory* 91(3):323–332. [PubMed: 19073269]
- Barg J, Levy R, Simantov R. 1984. Up-regulation of opiate receptors by opiate antagonists in neuroblastoma-glioma cell culture: the possibility of interaction with guanosine triphosphate-binding proteins. *Neuroscience Letters* 50(1–3):133–137. [PubMed: 6093009]

- Becker HC. 2017. Influence of stress associated with chronic alcohol exposure on drinking. *Neuropharmacology* 122:115–126. [PubMed: 28431971]
- Bie B, Zhang Z, Cai YQ, Zhu W, Zhang Y, Dai J, Lowenstein CJ, Weinman EJ, Pan ZZ. 2010. Nerve growth factor-regulated emergence of functional delta-opioid receptors. *The Journal of Neuroscience: The Official Journal of the Society for Neuroscience* 30(16):5617–5628.
- Bolan EA, Pan YX, Pasternak GW. 2004. Functional analysis of MOR-1 splice variants of the mouse mu opioid receptor gene Oprm. *Synapse (New York, NY)* 51(1):11–18.
- Bolan EA, Tallarida RJ, Pasternak GW. 2002. Synergy between mu opioid ligands: evidence for functional interactions among mu opioid receptor subtypes. *The Journal of Pharmacology and Experimental Therapeutics* 303(2):557–562. [PubMed: 12388636]
- Boudin H, Pelaprat D, Rostene W, Pickel VM, Beaudet A. 1998. Correlative ultrastructural distribution of neurotensin receptor proteins and binding sites in the rat substantia nigra. *The Journal of Neuroscience: The Official Journal of the Society for Neuroscience* 18(20):8473–8484. [PubMed: 9763490]
- Bruchas MR, Xu M, Chavkin C. 2008. Repeated swim stress induces kappa opioid-mediated activation of extracellular signal-regulated kinase 1/2. *Neuroreport* 19(14):1417–1422. [PubMed: 18766023]
- Burstein SR, Williams TJ, Lane DA, Knudsen MG, Pickel VM, McEwen BS, Waters EM, Milner TA. 2013. The influences of reproductive status and acute stress on the levels of phosphorylated delta opioid receptor immunoreactivity in rat hippocampus. *Brain Research* 1518:71–81. [PubMed: 23583481]
- Centers for Disease Control and Prevention. 2015. Drug overdose deaths hit record numbers in 2014 (Retrieved from) <https://www.cdc.gov/media/releases/2015/p1218-drug-overdose.html>
- Celio MR. 1990. Calbindin D-28k and parvalbumin in the rat nervous system. *Neuroscience* 35(2):375–475. [PubMed: 2199841]
- Celio MR, Baier W, Scharer L, de Viragh PA, Gerday C. 1988. Monoclonal antibodies directed against the calcium binding protein parvalbumin. *Cell Calcium* 9(2):81–86. [PubMed: 3383226]
- Commons KG, Milner TA. 1996. Cellular and subcellular localization of delta opioid receptor immunoreactivity in the rat dentate gyrus. *Brain Research* 738(2):181–195. [PubMed: 8955512]
- Commons KG, Milner TA. 1997. Localization of delta opioid receptor immunoreactivity in interneurons and pyramidal cells in the rat hippocampus. *The Journal of Comparative Neurology* 381(3):373–387. [PubMed: 9133574]
- Conrad CD, Galea LA, Kuroda Y, McEwen BS. 1996. Chronic stress impairs rat spatial memory on the Y maze, and this effect is blocked by tianeptine pretreatment. *Behavioral Neuroscience* 110(6):1321–1334. [PubMed: 8986335]
- Corbett AD, Paterson SJ, Kosterlitz HW. 1993. Selectivity of Ligands for Opioid Receptors. In: Herz A, Akil H, Simon EJ, editors. *Opioids*. Berlin, Heidelberg: Springer Berlin Heidelberg. p. 645–679.
- Crain BJ, Chang KJ, McNamara JO. 1986. Quantitative autoradiographic analysis of mu and delta opioid binding sites in the rat hippocampal formation. *The Journal of Comparative Neurology* 246(2):170–180. [PubMed: 3007584]
- Czeh B, Simon M, van der Hart MG, Schmelting B, Hesselink MB, Fuchs E. 2005. Chronic stress decreases the number of parvalbumin-immunoreactive interneurons in the hippocampus: prevention by treatment with a substance P receptor (NK1) antagonist. *Neuropsychopharmacology: Official Publication of the American College of Neuropsychopharmacology* 30(1):67–79. [PubMed: 15470372]
- Deutsch-Feldman M, Picetti R, Seip-Cammack K, Zhou Y, Kreek MJ. 2015. Effects of handling and vehicle injections on adrenocorticotrophic and corticosterone concentrations in Sprague-Dawley compared with Lewis rats. *Journal of the American Association for Laboratory Animal Science* 54(1):35–39. [PubMed: 25651089]
- Drake CT, Chavkin C, Milner TA. 2007. Opioid systems in the dentate gyrus. *Progress in Brain Research* 163:245–263. [PubMed: 17765723]
- Drake CT, Milner TA. 1999. Mu opioid receptors are in somatodendritic and axonal compartments of GABAergic neurons in rat hippocampal formation. *Brain Research* 849(1–2):203–215. [PubMed: 10592303]

- Drake CT, Milner TA. 2006. Mu opioid receptors are extensively co-localized with parvalbumin, but not somatostatin, in the dentate gyrus. *Neuroscience Letters* 403(1–2):176–180. [PubMed: 16716508]
- Fernandez-Monreal M, Brown TC, Royo M, Esteban JA. 2012. The balance between receptor recycling and trafficking toward lysosomes determines synaptic strength during long-term depression. *The Journal of Neuroscience: The Official Journal of the Society for Neuroscience* 32(38):13200–13205.
- Gonzales KL, Chapleau JD, Pierce JP, Kelter DT, Williams TJ, Torres-Reveron A, McEwen BS, Waters EM, Milner TA. 2011. The influences of reproductive status and acute stress on the levels of phosphorylated mu opioid receptor immunoreactivity in rat hippocampus. *Frontiers in Endocrinology* 2(18).
- Gulya K, Gehlert DR, Wamsley JK, Mosberg H, Hruby VJ, Yamamura HI. 1986. Light microscopic autoradiographic localization of delta opioid receptors in the rat brain using a highly selective bis-penicillamine cyclic enkephalin analog. *The Journal of Pharmacology and Experimental Therapeutics* 238(2):720–726. [PubMed: 3016247]
- Haberstock-Debic H, Wein M, Barrot M, Colago EE, Rahman Z, Neve RL, Pickel VM, Nestler EJ, von Zastrow M, Svingos AL. 2003. Morphine acutely regulates opioid receptor trafficking selectively in dendrites of nucleus accumbens neurons. *The Journal of Neuroscience: The Official Journal of the Society for Neuroscience* 23(10):4324–4332. [PubMed: 12764121]
- Haghighparast A, Fatahi Z, Alamdary SZ, Reisi Z, Khodaghohi F. 2014. Changes in the levels of p-ERK, p-CREB, and c-fos in rat mesocorticolimbic dopaminergic system after morphine-induced conditioned place preference: the role of acute and subchronic stress. *Cellular and molecular neurobiology* 34(2):277–288. [PubMed: 24292370]
- Han JS. 2003. Acupuncture: neuropeptide release produced by electrical stimulation of different frequencies. *Trends in Neurosciences* 26(1):17–22. [PubMed: 12495858]
- Harte-Hargrove LC, Varga-Wesson A, Duffy AM, Milner TA, Scharfman HE. 2015. Opioid Receptor-Dependent Sex Differences in Synaptic Plasticity in the Hippocampal Mossy Fiber Pathway of the Adult Rat. *The Journal of Neuroscience: The Official Journal of the Society for Neuroscience* 35(4):1723–1738. [PubMed: 25632146]
- He L, Fong J, von Zastrow M, Whistler JL. 2002. Regulation of opioid receptor trafficking and morphine tolerance by receptor oligomerization. *Cell* 108(2):271–282. [PubMed: 11832216]
- Hu M, Crombag HS, Robinson TE, Becker JB. 2004. Biological basis of sex differences in the propensity to self-administer cocaine. *Neuropsychopharmacology: Official Publication of the American College of Neuropsychopharmacology* 29(1):81–85. [PubMed: 12955098]
- Kesner RP, Warthen DK. 2010. Implications of CA3 NMDA and opiate receptors for spatial pattern completion in rats. *Hippocampus* 20(4):550–557. [PubMed: 19650123]
- Kieffer BL, Befort K, Gaveriaux-Ruff C, Hirth CG. 1992. The delta-opioid receptor: isolation of a cDNA by expression cloning and pharmacological characterization. *Proceedings of the National Academy of Sciences of the United States of America* 89(24):12048–12052. [PubMed: 1334555]
- Kitraki E, Kremmyda O, Youlatos D, Alexis MN, Kittas C. 2004. Gender-dependent alterations in corticosteroid receptor status and spatial performance following 21 days of restraint stress. *Neuroscience* 125(1):47–55. [PubMed: 15051144]
- Koob GF, Volkow ND. 2010. Neurocircuitry of addiction. *Neuropsychopharmacology: Official Publication of the American College of Neuropsychopharmacology* 35(1):217–238. [PubMed: 19710631]
- Lacy RT, Strickland JC, Feinstein MA, Robinson AM, Smith MA. 2016. The effects of sex, estrous cycle, and social contact on cocaine and heroin self-administration in rats. *Psychopharmacology* 233(17):3201–3210. [PubMed: 27370020]
- Lauder JM, Han VK, Henderson P, Verdoorn T, Towle AC. 1986. Prenatal ontogeny of the GABAergic system in the rat brain: an immunocytochemical study. *Neuroscience* 19(2):465–493. [PubMed: 3022187]
- Li Y, Li GY, Li LJ, Wang CH, Li ZX, Zhang JL, Zhang J, Li WH. 2007. Subsequently enhanced CPP to morphine following chronic but not acute footshock stress associated with corticosterone

- mechanism in rats. *The International Journal of Neuroscience* 117(9):1237–1255. [PubMed: 17654090]
- Liang J, Ping XJ, Li YJ, Ma YY, Wu LZ, Han JS, Cui CL. 2010. Morphine-induced conditioned place preference in rats is inhibited by electroacupuncture at 2 Hz: role of enkephalin in the nucleus accumbens. *Neuropharmacology* 58(1):233–240. [PubMed: 19596017]
- Luine VN, Beck KD, Bowman RE, Frankfurt M, Maclusky NJ. 2007. Chronic stress and neural function: accounting for sex and age. *Journal of Neuroendocrinology* 19(10):743–751. [PubMed: 17850456]
- Mansour A, Fox CA, Burke S, Meng F, Thompson RC, Akil H, Watson SJ. 1994. Mu, delta, and kappa opioid receptor mRNA expression in the rat CNS: an in situ hybridization study. *The Journal of Comparative Neurology* 350(3):412–438. [PubMed: 7884049]
- Mansour A, Khachaturian H, Lewis ME, Akil H, Watson SJ. 1987. Autoradiographic differentiation of mu, delta, and kappa opioid receptors in the rat forebrain and midbrain. *The Journal of Neuroscience: The Official Journal of the Society for Neuroscience* 7(8):2445–2464. [PubMed: 3039080]
- Mavrikaki M, Pravetoni M, Page S, Potter D, Chartoff E. 2017. Oxycodone self-administration in male and female rats. *Psychopharmacology* 234(6):977–987. [PubMed: 28127624]
- Mazid S, Hall BS, Odell SC, Stafford K, Dyer AD, Van Kempen TA, Selegan J, McEwen BS, Waters EM, Milner TA. 2016. Sex differences in subcellular distribution of delta opioid receptors in the rat hippocampus in response to acute and chronic stress. *Neurobiology of Stress* 5:37–53. [PubMed: 27981195]
- McEwen BS. 1999. Stress and hippocampal plasticity. *Annual Review of Neuroscience* 22:105–122.
- McEwen BS, Milner TA. 2007. Hippocampal formation: shedding light on the influence of sex and stress on the brain. *Brain Research Reviews* 55(2):343–355. [PubMed: 17395265]
- McEwen BS, Milner TA. 2017. Understanding the Broad Influence of Sex Hormones and Sex Differences in the Brain. *Journal of Neuroscience Research* 95(1–2):24–39. [PubMed: 27870427]
- McEwen BS, Nasca C, Gray JD. 2016. Stress Effects on Neuronal Structure: Hippocampus, Amygdala, and Prefrontal Cortex. *Neuropsychopharmacology: Official Publication of the American College of Neuropsychopharmacology* 41(1):3–23. [PubMed: 26076834]
- McLean S, Rothman RB, Jacobson AE, Rice KC, Herkenham M. 1987. Distribution of opiate receptor subtypes and enkephalin and dynorphin immunoreactivity in the hippocampus of squirrel, guinea pig, rat, and hamster. *The Journal of Comparative Neurology* 255(4):497–510. [PubMed: 2880880]
- Meilandt WJ, Barea-Rodriguez E, Harvey SA, Martinez JL Jr. 2004. Role of hippocampal CA3 mu-opioid receptors in spatial learning and memory. *The Journal of Neuroscience: The Official Journal of the Society for Neuroscience* 24(12):2953–2962. [PubMed: 15044534]
- Milner TA, Bacon CE. 1989a. GABAergic neurons in the rat hippocampal formation: ultrastructure and synaptic relationships with catecholaminergic terminals. *The Journal of Neuroscience: The Official Journal of the Society for Neuroscience* 9(10):3410–3427. [PubMed: 2795131]
- Milner TA, Bacon CE. 1989b. Ultrastructural localization of somatostatin-like immunoreactivity in the rat dentate gyrus. *The Journal of Comparative Neurology* 290(4):544–560. [PubMed: 2613944]
- Milner TA, Burstein SR, Marrone GF, Khalid S, Gonzalez AD, Williams TJ, Schierberl KC, Torres-Reveron A, Gonzales KL, McEwen BS, Waters EM. 2013. Stress differentially alters mu opioid receptor density and trafficking in parvalbumin-containing interneurons in the female and male rat hippocampus. *Synapse (New York, NY)* 67(11):757–772.
- Milner TA, Pickel VM, Reis DJ. 1989. Ultrastructural basis for interactions between central opioids and catecholamines. I. Rostral ventrolateral medulla. *The Journal of Neuroscience: The Official Journal of the Society for Neuroscience* 9(6):2114–2130. [PubMed: 2566665]
- Milner TA, Veznedaroglu E. 1992. Ultrastructural localization of neuropeptide Y-like immunoreactivity in the rat hippocampal formation. *Hippocampus* 2(2):107–125. [PubMed: 1308177]
- Milner TA, Waters EM, Robinson DC, Pierce JP. 2011. Degenerating processes identified by electron microscopic immunocytochemical methods. *Neurodegeneration, Methods and Protocols*:23–59.

- Moore SD, Madamba SG, Schweitzer P, Siggins GR. 1994. Voltage-dependent effects of opioid peptides on hippocampal CA3 pyramidal neurons in vitro. *The Journal of Neuroscience: The Official Journal of the Society for Neuroscience* 14(2):809–820. [PubMed: 7905518]
- Narita M, Nakamura A, Ozaki M, Imai S, Miyoshi K, Suzuki M, Suzuki T. 2008. Comparative pharmacological profiles of morphine and oxycodone under a neuropathic pain-like state in mice: evidence for less sensitivity to morphine. *Neuropsychopharmacology: Official Publication of the American College of Neuropsychopharmacology* 33(5):1097–1112. [PubMed: 17593930]
- Nielsen CK, Ross FB, Lotfipour S, Saini KS, Edwards SR, Smith MT. 2007. Oxycodone and morphine have distinctly different pharmacological profiles: radioligand binding and behavioural studies in two rat models of neuropathic pain. *Pain* 132(3):289–300. [PubMed: 17467904]
- Olive MF, Anton B, Micevych P, Evans CJ, Maidment NT. 1997. Presynaptic versus postsynaptic localization of mu and delta opioid receptors in dorsal and ventral striatopallidal pathways. *The Journal of Neuroscience: The Official Journal of the Society for Neuroscience* 17(19):7471–7479. [PubMed: 9295393]
- Olmstead MC, Burns LH. 2005. Ultra-low-dose naltrexone suppresses rewarding effects of opiates and aversive effects of opiate withdrawal in rats. *Psychopharmacology* 181(3):576–581. [PubMed: 16010543]
- Ordóñez Gallego A, González Baron M, Espinosa Arranz E. 2007. Oxycodone: a pharmacological and clinical review. *Clinical & Translational Oncology: Official Publication of the Federation of Spanish Oncology Societies and of the National Cancer Institute of Mexico* 9(5):298–307. [PubMed: 17525040]
- Papp M, Lappas S, Muscat R, Willner P. 1992. Attenuation of place preference conditioning but not place aversion conditioning by chronic mild stress. *Journal of Psychopharmacology (Oxford, England)* 6(3):352–356. [PubMed: 22291379]
- Persson AI, Thorlin T, Eriksson PS. 2005. Comparison of immunoblotted delta opioid receptor proteins expressed in the adult rat brain and their regulation by growth hormone. *Neuroscience Research* 52(1):1–9. [PubMed: 15811547]
- Peters A, Palay SL, Webster H.d. 1991. *The fine structure of the nervous system: neurons and their supporting cells*. New York: Oxford University Press.
- Pierce JP, Kelter DT, McEwen BS, Waters EM, Milner TA. 2014. Hippocampal mossy fiber leu-enkephalin immunoreactivity in female rats is significantly altered following both acute and chronic stress. *Journal of Chemical Neuroanatomy* 55:9–17. [PubMed: 24275289]
- Pierce JP, Kievits J, Graustein B, Speth RC, Iadecola C, Milner TA. 2009. Sex differences in the subcellular distribution of AT(1) receptors and nadph oxidase subunits in the dendrites of C1 neurons in the rat rostral ventrolateral medulla. *Neuroscience* 163(1):329–338. [PubMed: 19501631]
- Pierce JP, Kurucz OS, Milner TA. 1999. Morphometry of a peptidergic transmitter system: Dynorphin B-like immunoreactivity in the rat hippocampal mossy fiber pathway before and after seizures. *Hippocampus* 9(3):255–276. [PubMed: 10401641]
- Prus AJ, James JR, Rosecrans JA. 2009. *Frontiers in Neuroscience: Conditioned Place Preference*. In: nd, Buccafusco JJ, editors. *Methods of Behavior Analysis in Neuroscience*. Boca Raton (FL): CRC Press/Taylor & Francis Group, LLC.
- Randesi M, Zhou Y, Mazid S, Odell SC, Gray JD, Correa da Rosa J, McEwen BS, Milner TA, Kreek MJ. 2018. Sex differences after chronic stress in the expression of opioid- and neuroplasticity-related genes in the rat hippocampus. *Neurobiology of Stress* 8:33–41. [PubMed: 29888302]
- Ribeiro-Dasilva MC, Shinal RM, Glover T, Williams RS, Staud R, Riley JL 3rd, Fillingim RB. 2011. Evaluation of menstrual cycle effects on morphine and pentazocine analgesia. *Pain* 152(3):614–622. [PubMed: 21239109]
- Rozeske RR, Der-Avakian A, Bland ST, Beckley JT, Watkins LR, Maier SF. 2009. The medial prefrontal cortex regulates the differential expression of morphine-conditioned place preference following a single exposure to controllable or uncontrollable stress. *Neuropsychopharmacology: Official Publication of the American College of Neuropsychopharmacology* 34(4):834–843. [PubMed: 18368036]

- Ryan JD, Zhou Y, Contoreggi NH, Bshesh FK, Gray JD, Kogan JF, Ben KT, McEwen BS, Jeanne Kreek M, Milner TA. 2018. Sex differences in the rat hippocampal opioid system after oxycodone conditioned place preference. *Neuroscience* 393:236–257. [PubMed: 30316908]
- Saal D, Dong Y, Bonci A, Malenka RC. 2003. Drugs of abuse and stress trigger a common synaptic adaptation in dopamine neurons. *Neuron* 37(4):577–582. [PubMed: 12597856]
- Saland LC, Hastings CM, Abeyta A, Chavez JB. 2005. Chronic ethanol modulates delta and mu-opioid receptor expression in rat CNS: immunohistochemical analysis with quantitative confocal microscopy. *Neuroscience Letters* 381(1–2):163–168. [PubMed: 15882810]
- Scharfman HE, MacLusky NJ. 2014. Sex differences in the neurobiology of epilepsy: a preclinical perspective. *Neurobiology of Disease* 72 Pt B:180–192. [PubMed: 25058745]
- Shaham Y, Erb S, Stewart J. 2000. Stress-induced relapse to heroin and cocaine seeking in rats: a review. *Brain Research Reviews* 33(1):13–33. [PubMed: 10967352]
- Sinha R. 2007. The role of stress in addiction relapse. *Current Psychiatry Reports* 9(5):388–395. [PubMed: 17915078]
- Sjulson L, Peyrache A, Cumpelik A, Cassataro D, Buzsaki G. 2018. Cocaine place conditioning strengthens location-specific hippocampal coupling to the nucleus accumbens. *Neuron* 98: 926–934. [PubMed: 29754750]
- Sousa N, Lukoyanov NV, Madeira MD, Almeida OF, Paula-Barbosa MM. 2000. Reorganization of the morphology of hippocampal neurites and synapses after stress-induced damage correlates with behavioral improvement. *Neuroscience* 97(2):253–266. [PubMed: 10799757]
- Sperk G, Hamilton T, Colmers WF. 2007. Neuropeptide Y in the dentate gyrus. *Progress in Brain Research* 163:285–297. [PubMed: 17765725]
- Stewart J. 2003. Stress and relapse to drug seeking: studies in laboratory animals shed light on mechanisms and sources of long-term vulnerability. *The American Journal on Addictions* 12(1):1–17. [PubMed: 12623736]
- Stumm RK, Zhou C, Schulz S, Hollt V. 2004. Neuronal types expressing mu- and delta-opioid receptor mRNA in the rat hippocampal formation. *The Journal of Comparative Neurology* 469(1):107–118. [PubMed: 14689476]
- Swanson LW. 1992. *Brain Maps: Structure of the Rat Brain*. Amsterdam: Elsevier.
- Torres-Reveron A, Khalid S, Williams TJ, Waters EM, Drake CT, McEwen BS, Milner TA. 2008. Ovarian steroids modulate leu-enkephalin levels and target leu-enkephalinergic profiles in the female hippocampal mossy fiber pathway. *Brain Research* 1232:70–84. [PubMed: 18691558]
- Torres-Reveron A, Khalid S, Williams TJ, Waters EM, Jacome L, Luine VN, Drake CT, McEwen BS, Milner TA. 2009a. Hippocampal dynorphin immunoreactivity increases in response to gonadal steroids and is positioned for direct modulation by ovarian steroid receptors. *Neuroscience* 159(1):204–216. [PubMed: 19150393]
- Torres-Reveron A, Williams TJ, Chapleau JD, Waters EM, McEwen BS, Drake CT, Milner TA. 2009b. Ovarian steroids alter mu opioid receptor trafficking in hippocampal parvalbumin GABAergic interneurons. *Experimental Neurology* 219(1):319–327. [PubMed: 19505458]
- Turner CD, Bagnara JT. 1971. *General Endocrinology*. Philadelphia: W.B. Saunders.
- Van Kempen TA, Gorecka J, Gonzalez AD, Soeda F, Milner TA, Waters EM. 2014. Characterization of Neural Estrogen Signaling and Neurotrophic Changes in the Accelerated Ovarian Failure Mouse Model of Menopause. *Endocrinology* 155(9):3610–3623. [PubMed: 24926825]
- Walker QD, Cabassa J, Kaplan KA, Li ST, Haroon J, Spohr HA, Kuhn CM. 2001. Sex differences in cocaine-stimulated motor behavior: disparate effects of gonadectomy. *Neuropsychopharmacology: Official Publication of the American College of Neuropsychopharmacology* 25(1):118–130. [PubMed: 11377925]
- Walker QD, Nelson CJ, Smith D, Kuhn CM. 2002. Vaginal lavage attenuates cocaine-stimulated activity and establishes place preference in rats. *Pharmacology, Biochemistry, and Behavior* 73(4):743–752. [PubMed: 12213518]
- Williams TJ, Milner TA. 2011. Delta opioid receptors colocalize with corticotropin releasing factor in hippocampal interneurons. *Neuroscience* 179:9–22. [PubMed: 21277946]

- Williams TJ, Torres-Reveron A, Chapleau JD, Milner TA. 2011. Hormonal regulation of delta opioid receptor immunoreactivity in interneurons and pyramidal cells in the rat hippocampus. *Neurobiology of Learning and Memory* 95(2):206–220. [PubMed: 21224009]
- Wong M, Moss RL. 1992. Long-term and short-term electrophysiological effects of estrogen on the synaptic properties of hippocampal CA1 neurons. *The Journal of Neuroscience: The Official Journal of the Society for Neuroscience* 12(8):3217–3225. [PubMed: 1353794]
- Znamensky V, Akama KT, McEwen BS, Milner TA. 2003. Estrogen Levels Regulate the Subcellular Distribution of Phosphorylated Akt in Hippocampal CA1 Dendrites. *The Journal of Neuroscience* 23(6):2340–2347. [PubMed: 12657693]
- Zupanc GK. 1996. Peptidergic transmission: from morphological correlates to functional implications. *Micron (Oxford, England)* 27(1):35–91.

Sex differences in the rat hippocampal opioid system






Opioid marker	region	Unstressed		CIS		Saline CPP		Oxy CPP	
		female*	male	female*	male	female^	male	female^	male
 L-Enk levels	MF-CA3b		>		>		>		=
 DORs in CA3 pyramidal cell dendrites	on PM				>				
	near PM		>				<		=
	cyto				<				<
 DOR spines	MF-CA3		>		>		=		=
 DORs in GABA dendrites	on PM						>		>
	near PM				>				>
	cyto								
 MORs in PARV dendrites	on PM		>		>		<		=
	near PM						<		=
	cyto				>		<		

Fig. 1. Summary of sex differences in the opioid system following CIS and oxycodone CPP in the rat hippocampus.

Our previous light and electron microscopic studies have revealed notable sex-differences in mossy fiber LEnk levels and in the redistributions of DORs and MORs in pyramidal cells and GABAergic interneurons following CIS and oxycodone CPP (Mazid et al., 2016; McEwen and Milner, 2017; Ryan et al., 2018). *Females in diestrus; ^Females in estrus.

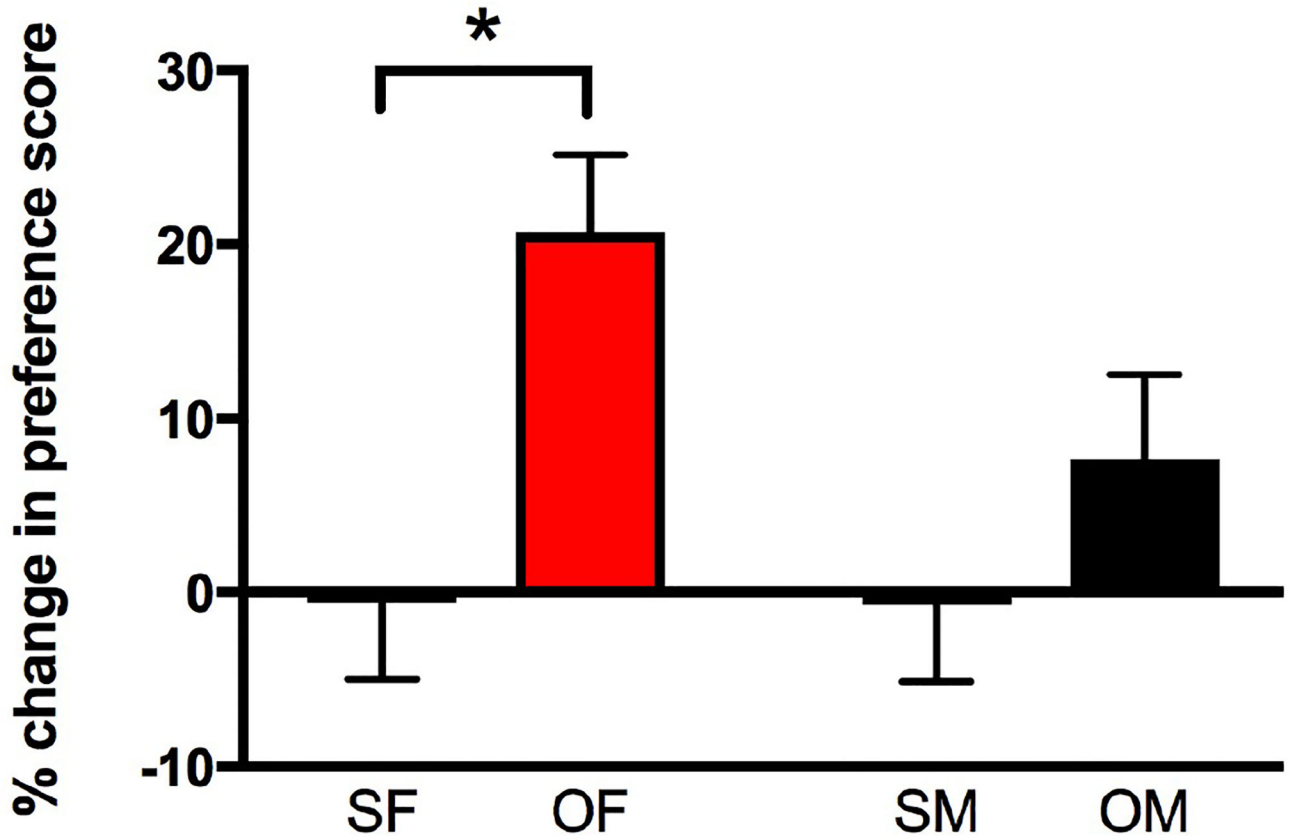


Fig. 2. Female but not male CIS rats develop oxycodone CPP.

A. During the preconditioning phase, female and male CIS rats displayed a pre-test preference for the white side of the chamber. Thus, a biased CPP design was used in which rats were placed in the least-preferred side following the oxycodone injection. On the testing day, saline-injected (Sal) rats showed no preference for either chamber. However, the percent change in preference score for the oxycodone-injected (Oxy) chamber is higher in CIS female rats compared to their Sal counterparts. Oxy-CIS males did not show a significantly greater preference for the oxycodone chamber than their saline-injected counterparts. SF, Sal-female; SM, Sal-male; OF, Oxy-female; OM, Oxy-male. * $p < 0.05$; $N = 6$ rats per group.

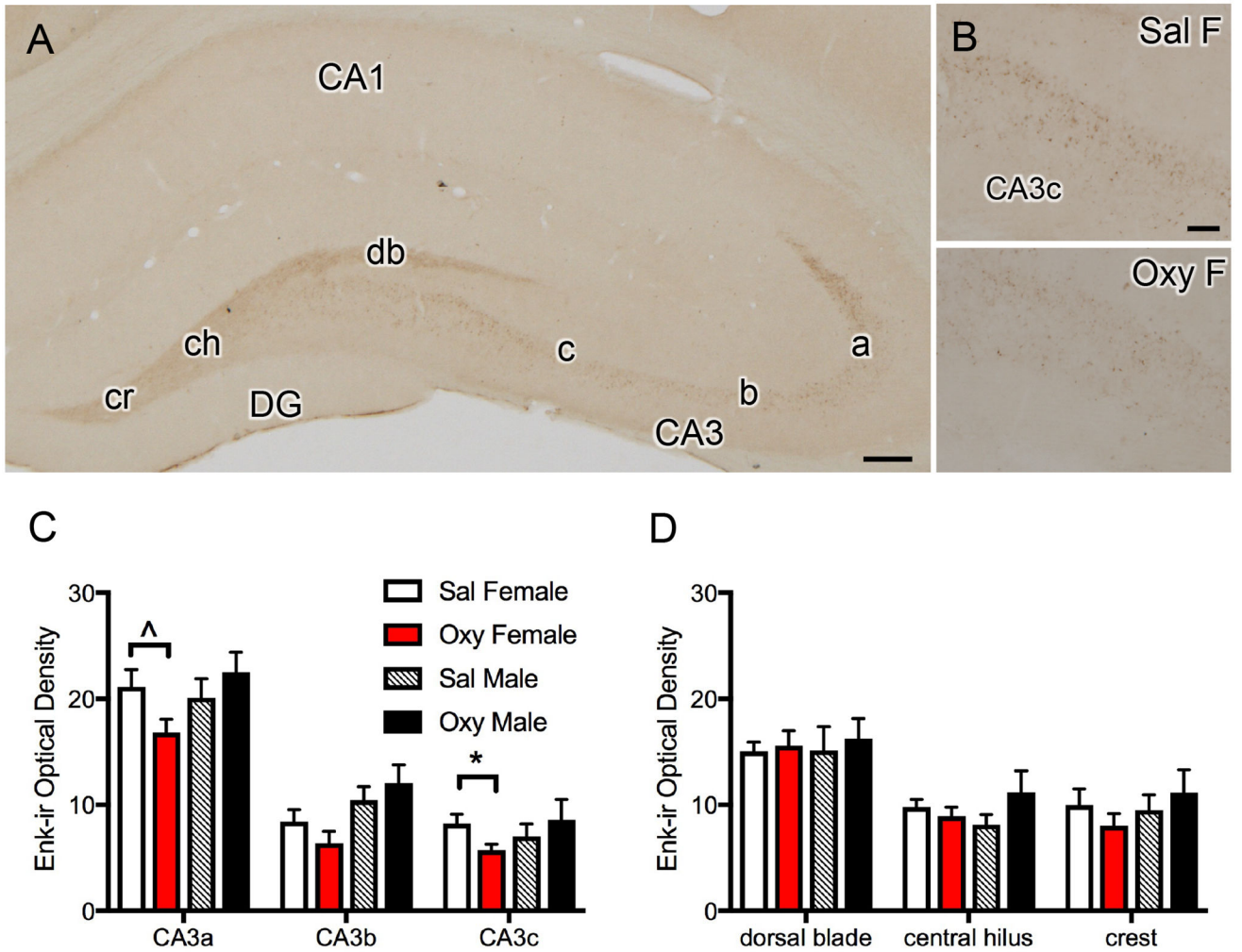


Fig. 3. LEnk levels in CA3 are modestly reduced in Oxy-CIS females.

A. Low magnification photomicrograph of the rat dorsal hippocampus shows LEnk-ir in the mossy fiber pathway within stratum lucidum (SLu) of CA3a, b and c and in the crest (cr), central hilus (ch), and dorsal blade (db) of the dentate gyrus (DG). **B.** High magnification photomicrographs show higher levels of LEnk-ir in CA3c SLu in a Sal-CIS female rat compared to an Oxy-CIS female rat. **C.** Oxy-CIS females compared to Sal-CIS females demonstrate decreased levels of LEnk-ir in the CA3c and a trend towards decreased levels of LEnk-ir in the CA3a. Oxy-CIS males compared to Sal-CIS males show no difference in levels of LEnk-ir in the CA3. **D.** Oxy-CIS females and males compared to Sal-CIS females and males show no difference in levels of LEnk-ir in any subregion of the DG. * $p < 0.05$; $\wedge p = 0.069$; $N = 6$ rats per group. Scale bars: A = 500 μm ; B = 100 μm

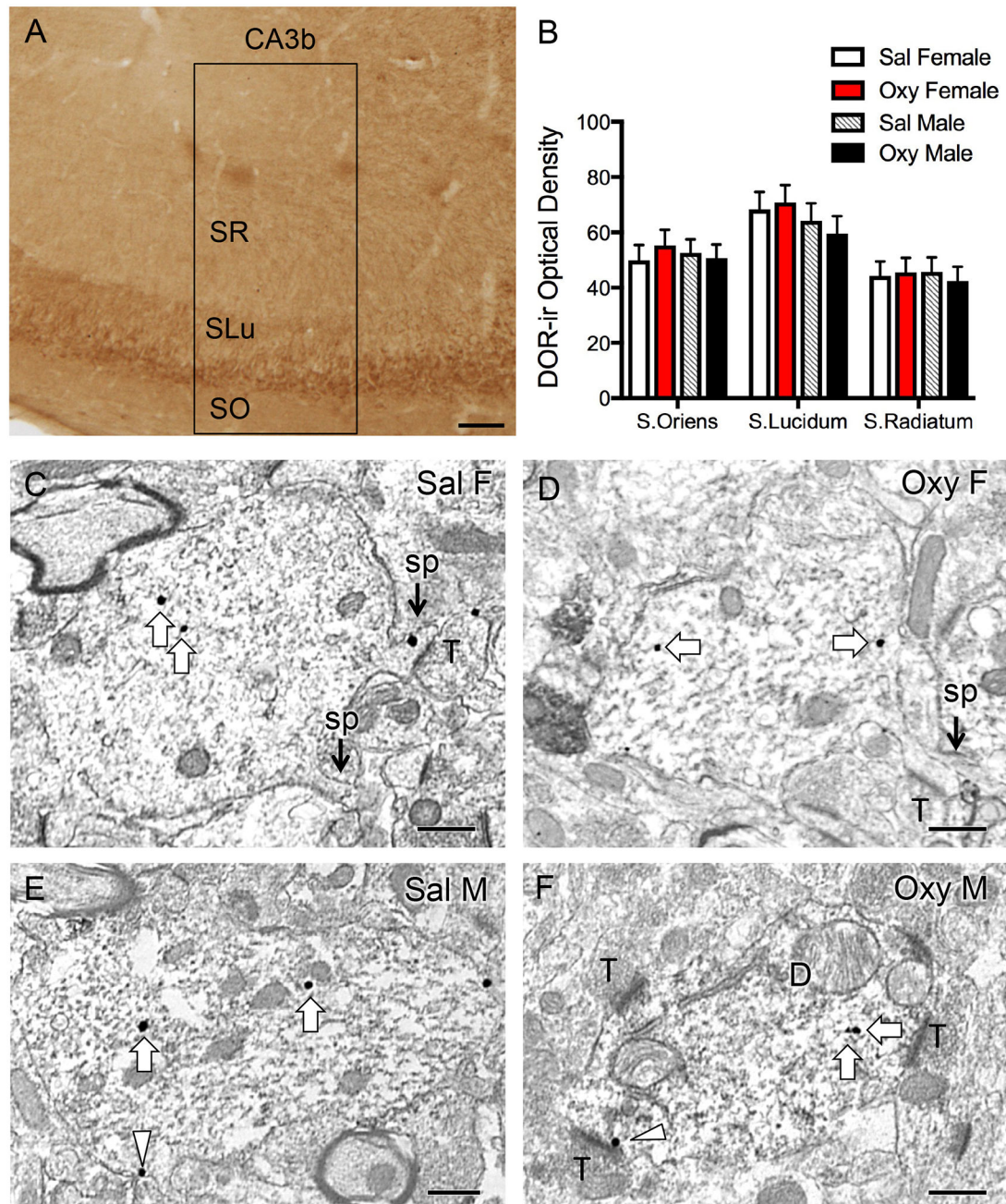


Fig. 4. Representative light and electron micrographs of delta opioid receptor (DOR) in CA3 pyramidal cell dendrites from Sal- and Oxy-CIS female and male rats.

A. Low magnification photomicrograph shows DOR-ir in the CA3 region of the dorsal hippocampus; box indicates area of CA3b sampled for densitometry and EM studies. SO, stratum oriens; SLu, stratum lucidum; SR, stratum radiatum. **B.** There is no significant difference in DOR-ir levels in any of the subregions of CA3b between Sal-CIS and Oxy-CIS female and male rats. $N = 6$ rats per group. **C-F.** Electron micrographs show the distribution of DOR-SIG particles within CA3 pyramidal cell dendrites from a Sal-CIS female (**C**), an Oxy-CIS female (**D**), a Sal-CIS male (**E**), and an Oxy-CIS male (**F**) rat. Examples of

near plasmalemmal (triangle) and cytoplasmic (arrow) DOR-SIG particles in dendrites are shown. CA3 dendrites often have spines (sp) that are contacted by terminals (T; example C). Scale bars: 100 μm (A); 500 nm (C-F).

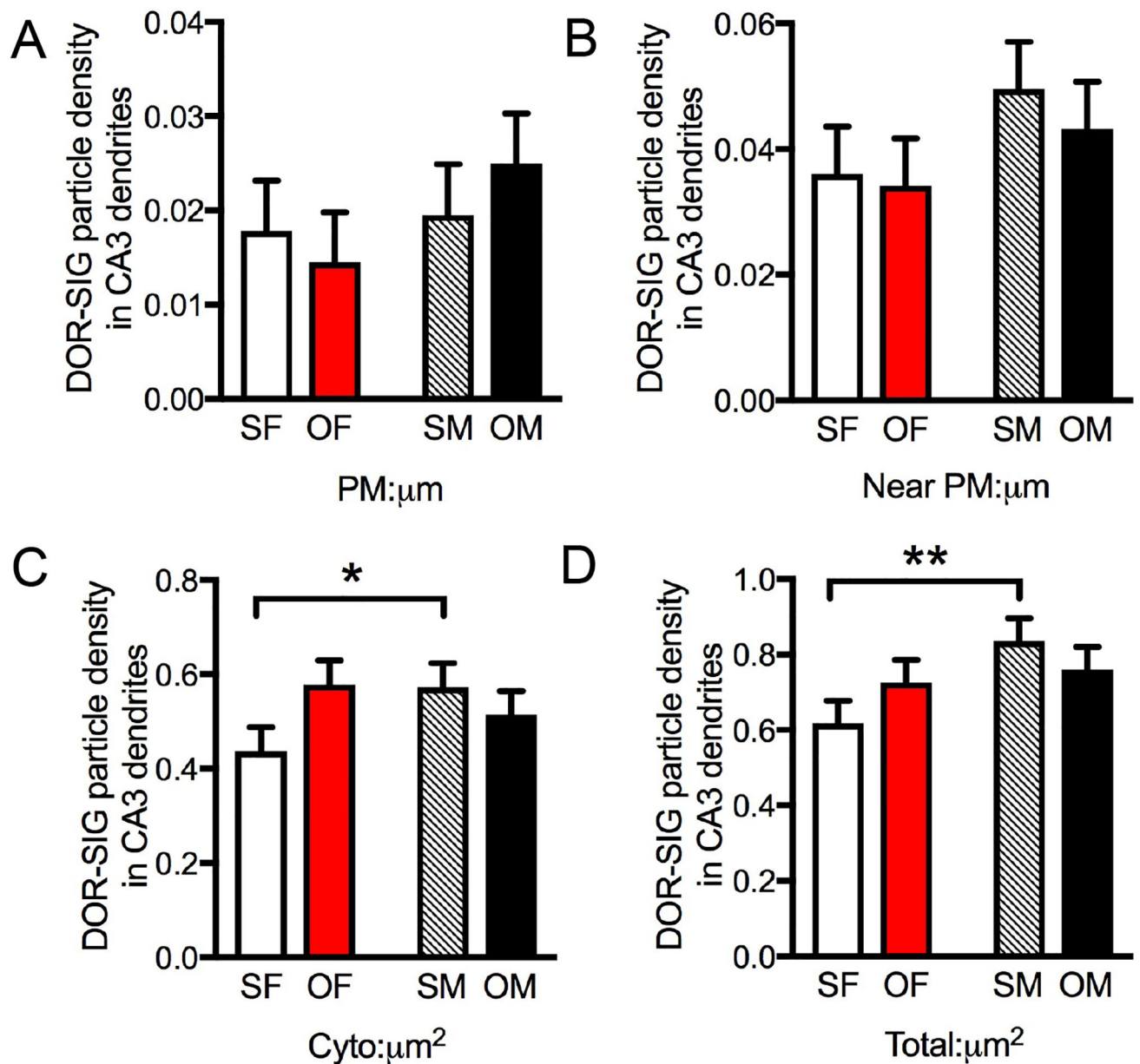


Fig. 5. Sex differences in the distribution of DOR-SIG particles in CA3 pyramidal cell dendrites in Sal- and Oxy-CIS female and male rats.

A,B. There are no differences in plasmalemmal or near plasmalemmal DOR-SIG particle density in CA3 dendrites between Sal- and Oxy-CIS females and males. **C,D.** Sal-CIS females have a significantly lower density of DOR-SIG particles in the cytoplasm and in total in CA3 pyramidal cell dendrites compared to Sal-CIS males. SF, Sal-female; SM, Sal-male; OF, Oxy-female; OM, Oxy-male. ** $p < 0.01$, * $p = 0.05$; $N = 3$ rats per group; $n = 50$ dendrites per rat.

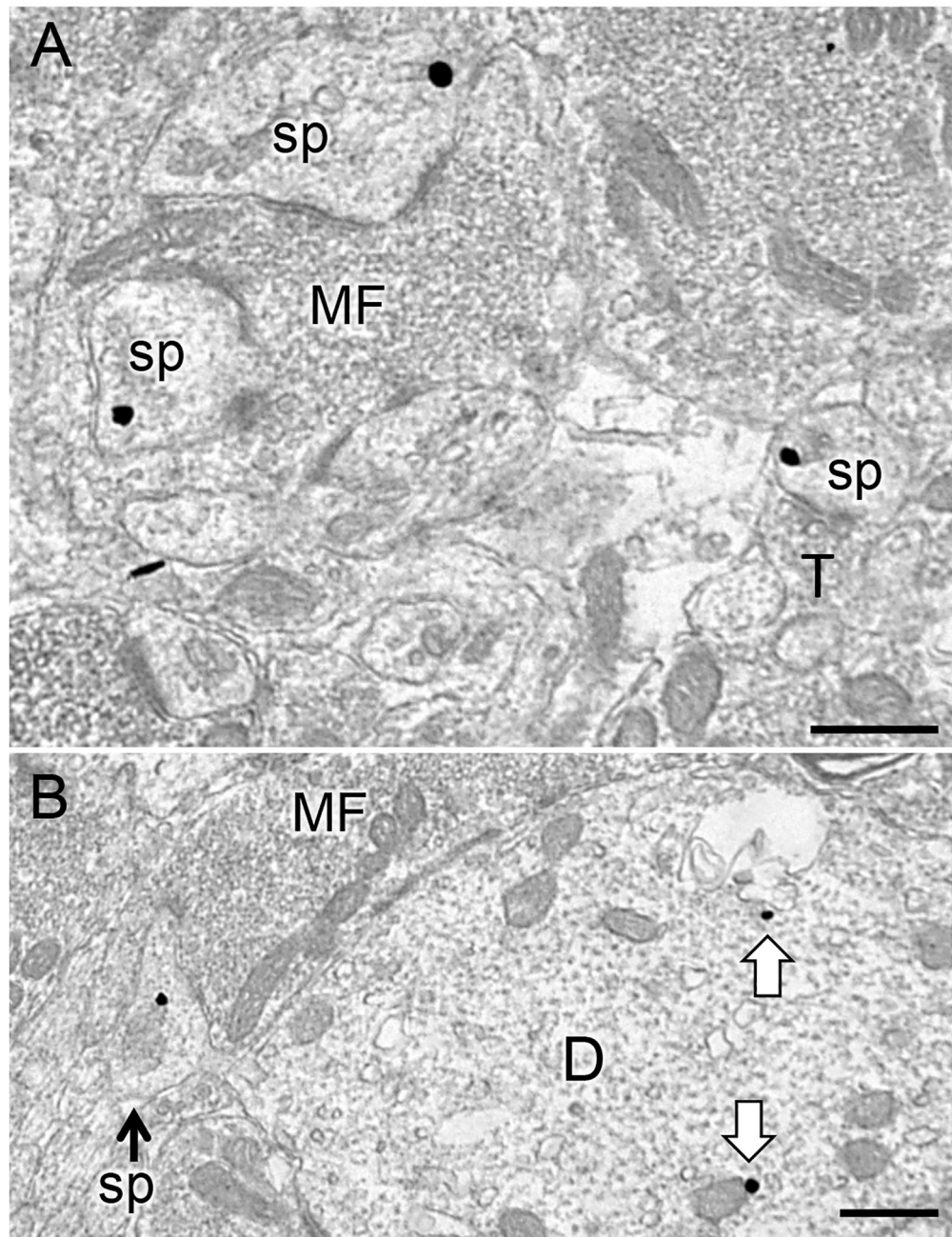


Fig. 6. Representative electron micrographs of DOR-labeled dendritic spines in SLu of CA3. **A.** DOR-SIG particles in the cytoplasm of two dendritic spines (sp) in contact with a mossy fiber (MF) in the CA3. Nearby, a DOR-SIG particle is found near the plasmalemma of a spine contacted by a terminal (T; bottom right). **B.** A DOR-SIG labeled spine emanates from a pyramidal cell dendrite with DOR-SIG particles in the cytoplasm (arrows). A MF abuts the DOR-labeled dendrite (D). Electron micrographs are from Oxy-CIS females. Scale bars: 500 nm.

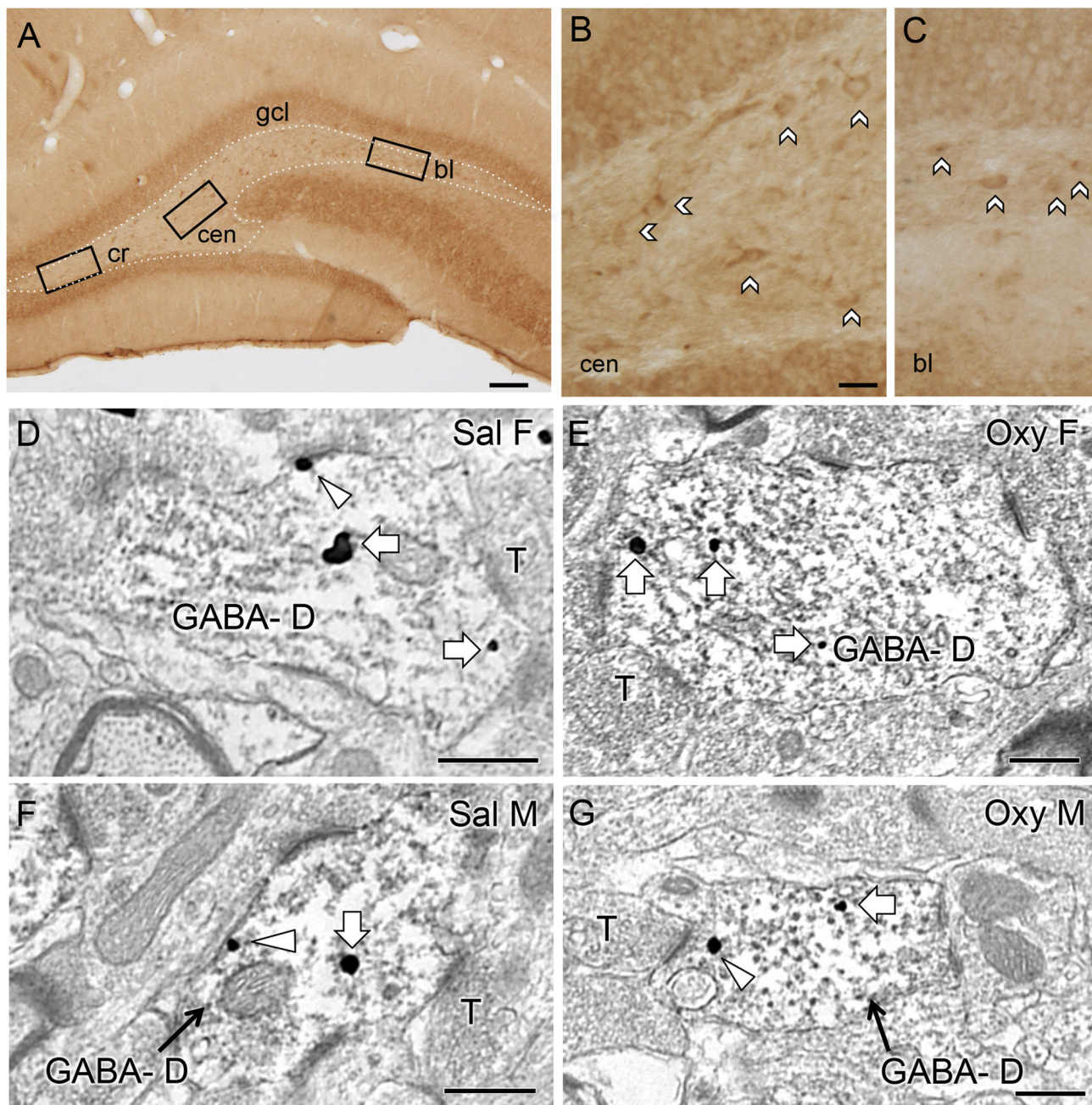


Fig. 7. Representative light and electron micrographs of delta opioid receptor (DOR) in the hilus of the dentate gyrus from Sal- and Oxy-CIS female and male rats.

A. Low magnification photomicrograph shows DOR-containing cells in three regions of the hilus in a CIS female rat (cr = crest; cen = central hilus; bl = blade). **B,C.** High magnification photomicrographs of the central hilus (**B**) and dorsal blade (**C**) show samples of DOR-labeled cells. No differences were observed in the number of DOR-labeled cells in any region of the hilus between Sal-CIS and Oxy-CIS female and male rats (see Table 2). **D-G.** Electron micrographs show the distribution of DOR-SIG particles within GABA-labeled dendrites (GABA-D) in the hilus from a Sal-CIS female (**D**), an Oxy-CIS female (**E**), a

Sal-CIS male (**F**) and an Oxy-CIS male (**G**) rat. Examples of near plasmalemmal (triangle) and cytoplasmic (arrow) DOR-SIG particles in dendrites are shown. Scale bars: 100 μm (**A**); 50 μm (**B**); 500 nm (**D-G**).

Author Manuscript

Author Manuscript

Author Manuscript

Author Manuscript

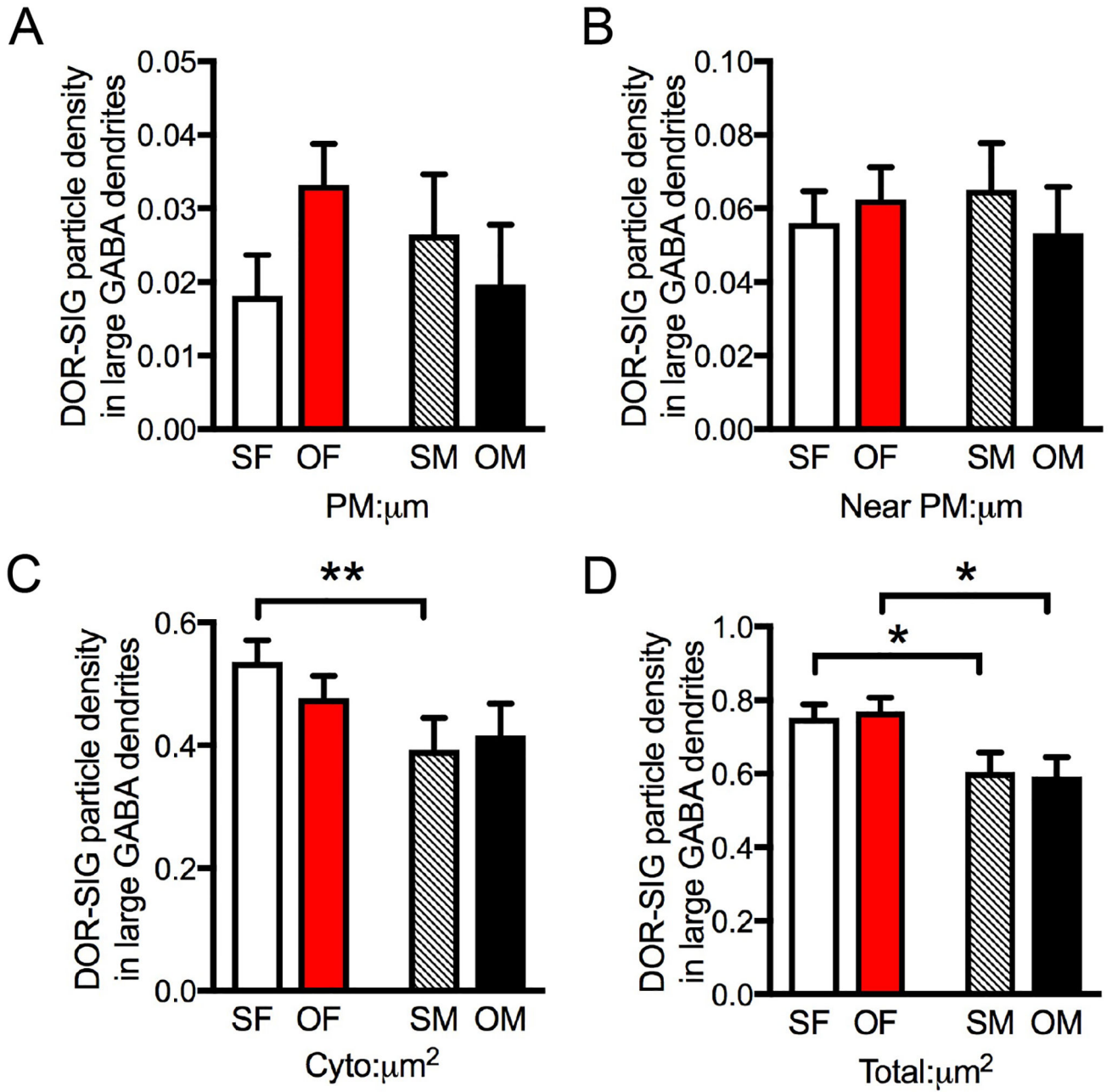


Fig. 8. Sex differences in the distribution of DOR-SIG particles in GABAergic hilar dendrites in Sal- and Oxy-CIS female and male rats.

A,B. There are no differences in plasmalemmal or near plasmalemmal DOR-SIG particle density between Sal- and Oxy-CIS females and males. **C,D.** Sal-CIS females compared to Sal-CIS males have a greater density of DOR-SIG particles in the cytoplasm (**C**) and in total (**D**) in large GABA-labeled dendrites. Sal-CIS females compared to Sal-CIS males have a greater density of DOR-SIG particles in total in small GABA-labeled dendrites (not shown). Oxy-CIS females compared to Oxy-CIS males have increased density of DOR-SIG particles in large (**D**) GABA-labeled dendrites. SF, Sal-female; SM, Sal-male; OF, Oxy-female; OM, Oxy-male. ** $p < 0.01$, * $p = 0.05$; $N = 3$ rats per group; $n = 50$ dendrites per rat.

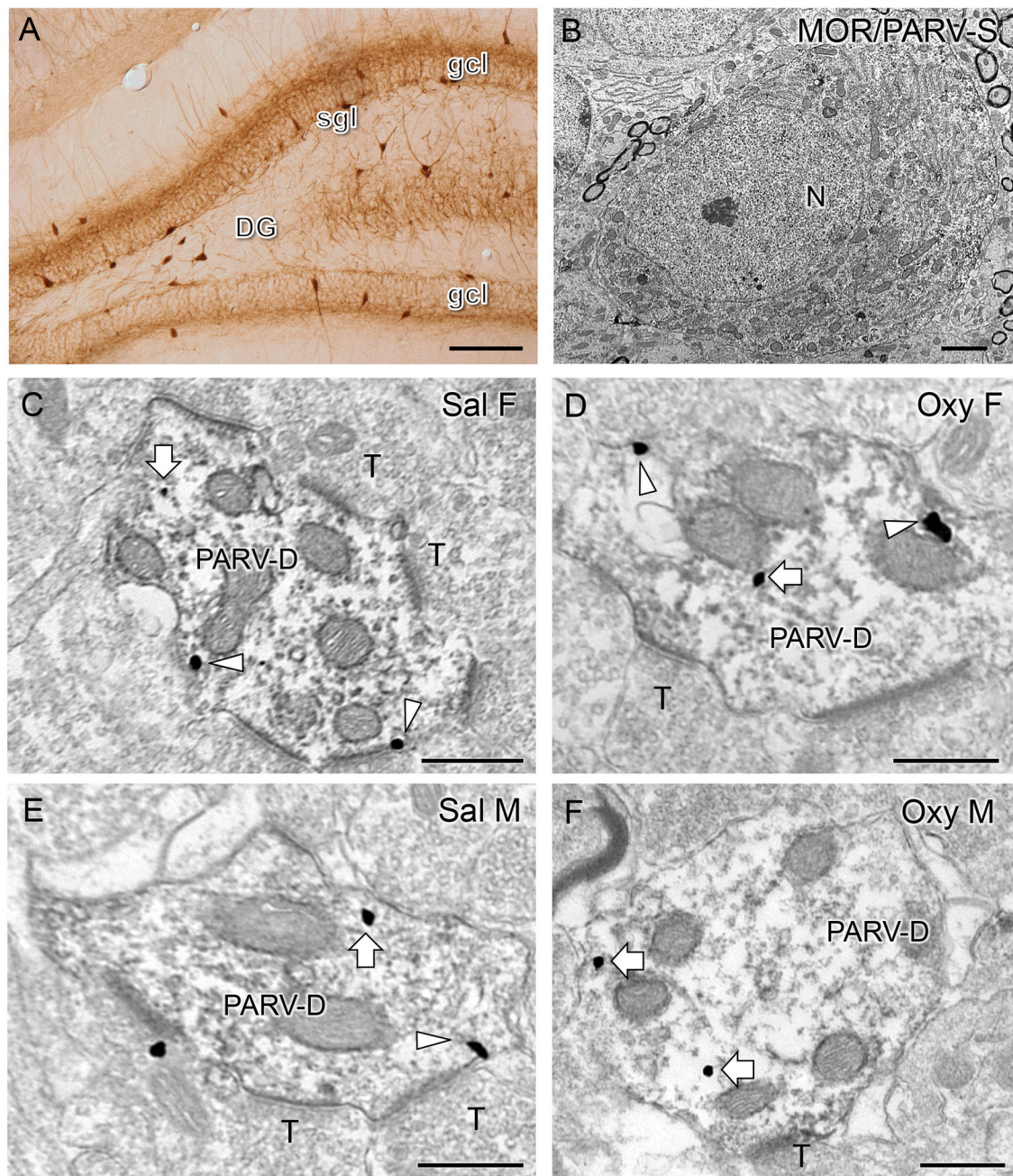


Fig. 9. Representative micrographs of MOR-SIG particles in PARV-containing interneurons in the hilus of the dentate gyrus from Sal- and Oxy-CIS rats.

A. Low magnification light microscopic photomicrograph shows PARV-labeled cells are primarily located in the subgranular region of the dentate gyrus (gcl = granule cell layer).

B. Electron micrograph shows example of a somata in the subgranular zone of the hilus dually labeled for MOR (SIG particles) and PARV (immunoperoxidase; N = nucleus).

C-F. Electron micrographs show the distribution of MOR-SIG particles within peroxidase-labeled PARV dendrites in the DG from a Sal-CIS female (**C**), an Oxy-CIS female (**D**), a Sal-CIS male (**E**), and an Oxy-CIS male (**F**) rat. Triangles and arrows indicate near

plasmalemmal and cytoplasmic MOR-SIG particles, respectively. PARV-labeled dendrites are often contacted by unlabeled terminals (T). Scale bars: 500 μm (**A**); 500 nm (**B-F**).

Author Manuscript

Author Manuscript

Author Manuscript

Author Manuscript

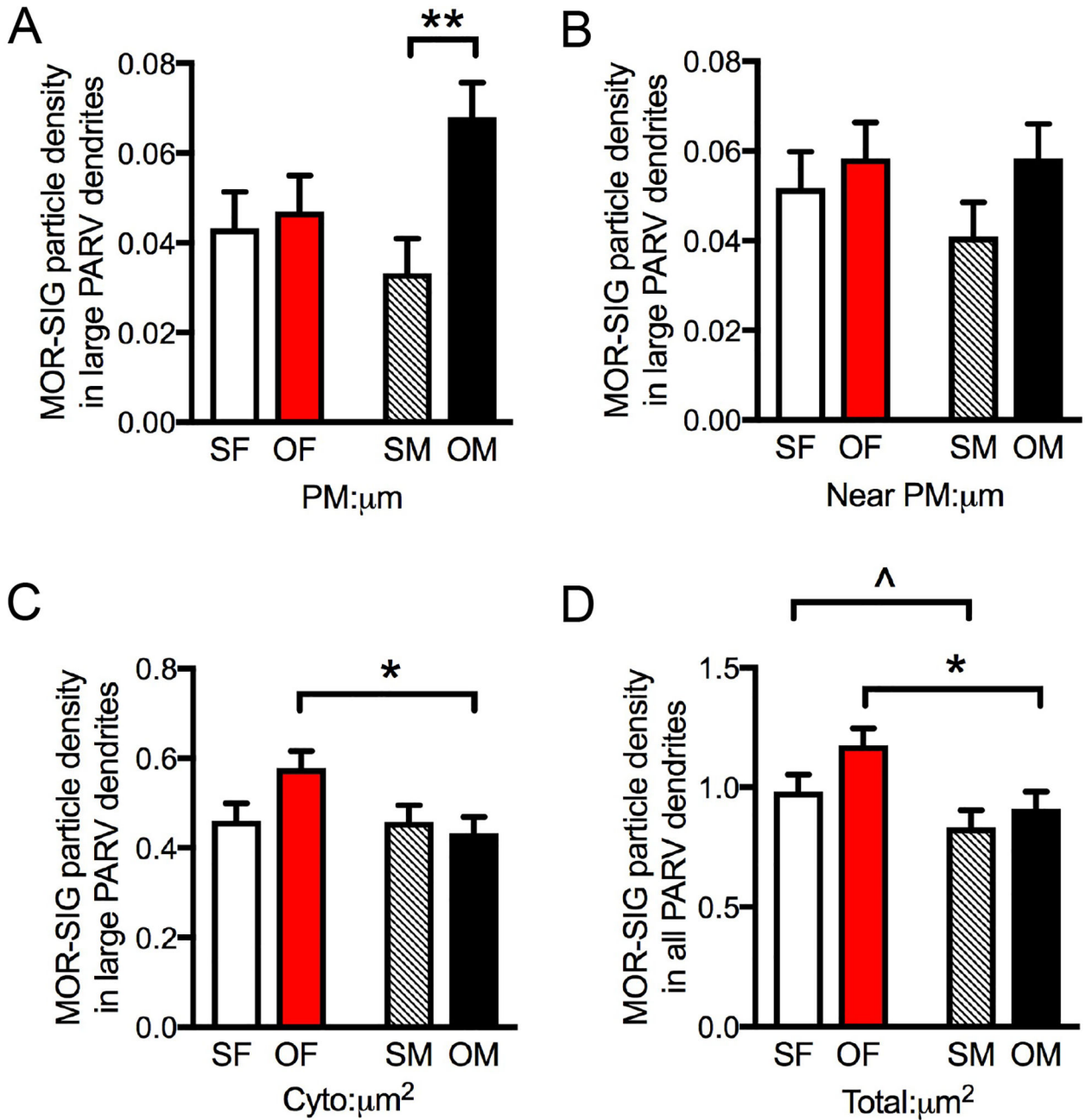


Fig. 10. Sex differences in the distribution of MOR-SIG particles in hilar parvalbumin (PARV)-labeled dendrites in Sal- and Oxy-CIS female and male rats.

A. In large PARV-labeled dendrites, Oxy-CIS males showed increased density of plasmalemmal MOR-SIG particles compared to Sal-CIS males. **B.** No significant differences between groups were observed in near plasmalemmal MOR-SIG particles in large PARV-labeled dendrites. **C.** In large PARV-labeled dendrites, Oxy-CIS females showed increased density of cytoplasmic MOR-SIG particles compared to Oxy-CIS males. **D.** Sal-CIS females compared to Sal-CIS males had a trend toward higher total densities of MOR-SIG particles in total PARV-labeled dendrites. Additionally, compared to Oxy-CIS males, Oxy-CIS

females showed a significant increase in total MOR-SIG particle density within total PARV-labeled dendrites. SF, Sal-female; SM, Sal-male; OF, Oxy-female; OM, Oxy-male. **p < 0.01, *p = 0.05, ^p = 0.066; N = 3 rats per group; n = 50 dendrites per rat.

Author Manuscript

Author Manuscript

Author Manuscript

Author Manuscript

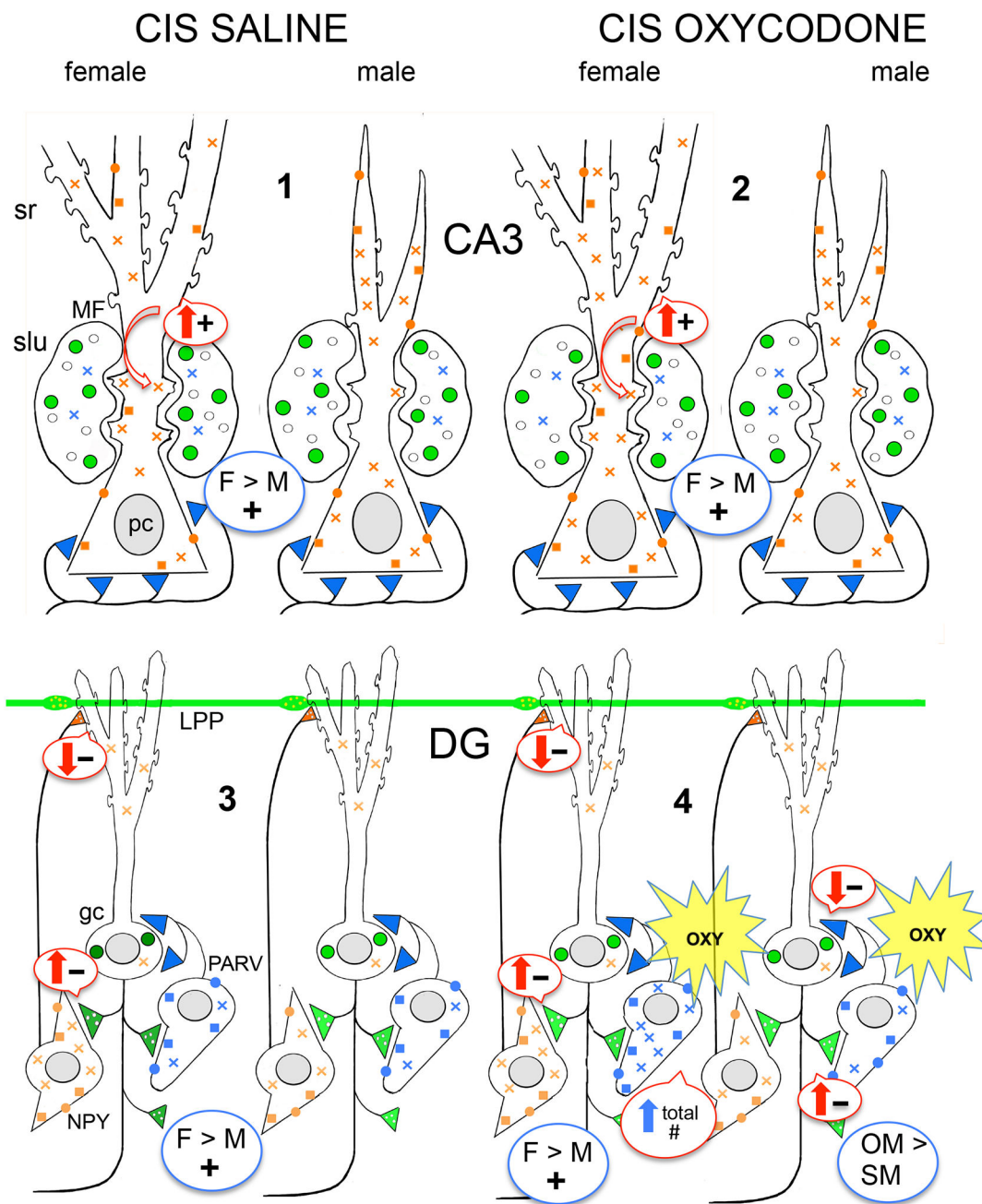


Fig. 11. Schematic illustrating sex differences in the hippocampal opioid system in Sal- and Oxy-CIS rats.

Arrows indicate predicted effects (upward = increased; downward = decreased) of DOR and MOR trafficking changes on excitation (plus signs) and inhibition (minus signs) in the CA3 and dentate gyrus (DG). #1-4 indicate points where there are differences in the distribution of DORs and MORs in Sal- and Oxy-CIS rats. gc, granule cell; hil, hilus; LPP, lateral perforant path; MF, mossy fiber; pc, pyramidal cell; slu, stratum lucidum; sr, stratum radiatum. Blue color = MORs; Green color = LEnk levels; orange color = DORs. Circles = plasmalemmal receptors; squares = near-plasmalemmal receptors; crosses = cytoplasmic receptors.

- 1.** Consistent with previous studies (Mazid et al., 2016; Pierce et al., 2014), the levels of LENk in mossy fibers are comparable in Sal-CIS females and Sal-CIS males. Sal-CIS females compared to Sal-CIS males have fewer cytoplasmic and total DORs in CA3b pyramidal cell dendrites. However, Sal-CIS females compared to Sal-CIS males have more DORs in mossy fiber – CA3 synapses suggesting mechanisms for promoting opioid-mediated LTP are still in place in females following CIS. Prior studies have shown that CIS results in the retraction of CA3 dendrites in male rats (McEwen, 1999).
 - 2.** CA3b mossy fiber LENk levels in both Oxy-CIS females and Oxy-CIS males are unaltered compared to Sal-CIS rats. In Oxy-CIS females, the density of cytoplasmic and total DORs in CA3 dendrites increases so that they are comparable to that seen in Sal- and Oxy-CIS males. Moreover, the density of DORs in mossy fiber – CA3 synapses remains elevated in Oxy-CIS females and remains low in Oxy-CIS males. These findings indicate that the redistribution of DORs in CA3 pyramidal cells in CIS females is similar to that reported previously in unstressed females (Ryan et al., 2018).
 - 3.** Sal-CIS females compared to Sal-CIS males have elevated cytoplasmic and total DORs in the dendrites of GABAergic-labeled interneurons previously shown to colocalize SOM/NPY (Commons and Milner, 1996; Williams and Milner, 2011). These findings suggest a greater capacity for synthesis or storage of DORs in GABAergic interneurons. Sal-females compared to Sal-males have no differences in the density of MORs in any compartment in the dendrites of PARV-containing interneurons. However, prior studies have shown that the number of PARV-labeled interneurons is reduced by about 30% in males, but not females, following CIS (Czeh et al., 2005; Hu et al., 2004; Milner et al., 2013), suggesting that the redistribution of MORs occurs in a subset of PARV interneurons.
 - 4.** Cytoplasmic and total DORs in GABA-labeled dendrites remain elevated in Oxy-CIS females compared to Oxy-CIS males. The number of dual labeled MOR/PARV cells is decreased in Oxy-CIS females compared to Sal-CIS females. However, the cytoplasmic and total density of MORs is elevated in Oxy-CIS females compared to Sal-CIS females, suggesting a greater capacity for synthesis or storage of MORs in a subset of PARV interneurons. In Oxy-CIS males compared to Sal-CIS males, plasmalemmal MORs are elevated in large PARV-labeled dendrites, suggesting that a subset of PARV neurons could have greater disinhibitory responses to MOR agonists.
- Together, these results demonstrate that CIS females, but not males, acquire CPP to oxycodone and CIS “primes” the hippocampal opioid system in females for oxycodone-associated learning. They also suggest that low levels of DORs in mossy fiber – CA3 synapses and hilar GABAergic interneurons may contribute to the lack of displayed oxycodone CPP in CIS males.

Table 1.**DOR-labeled spines in CA3 from CIS rats.**

CIS Group	% \pm SEM labeled spines	Location		
		synapse	membrane	cytoplasm
Stratum Lucidum				
Male Sal	2.6 \pm 0.8	0	1	8
Male Oxy	1.8 \pm 0.6 *	1	0	6
Female Sal	8.1 \pm 1.8	1	13	18
Female Oxy	11.5 \pm 3.3 *	2	18	21
Stratum Radiatum				
Male Sal	2.0 \pm 0.6	1	1	4
Male Oxy	3.3 \pm 0.9	2	3	7
Female Sal	5.3 \pm 2.3	2	6	8
Female Oxy	4.7 \pm 1.2	2	5	7

* Some spines had more than one DOR-SIG particle. Stratum lucidum: number of spines determined from 50 mossy fibers per rat per condition. Stratum radiatum: 100 spines randomly chosen per rat per condition. *p < 0.05

Table 2.

Number of DOR labeled cells in dentate gyrus

CIS Group	Total hilus	crest	central	Dorsal blade
Male Sal	23.5 ± 1.72	20.8 ± 4.73	20.0 ± 7.53	21.1 ± 4.77
Male Oxy	27.5 ± 2.80	22.5 ± 4.23	21.7 ± 2.11	22.2 ± 4.36
Female Sal	25.8 ± 3.11	20.8 ± 5.23	15.8 ± 4.36	22.2 ± 1.41
Female Oxy	24.8 ± 3.33	22.5 ± 3.82	14.2 ± 3.52	22.8 ± 3.80

The area of the hilus was measured using the granule cell layer and CA3 pyramidal cell layer as borders, and the number of cells per mm² was then calculated. The number of cells in the crest, central hilus and dorsal blade of the hilus was determined by randomly placing a 200 μm² rectangle over these regions, using the granule cell layer as a guide.